AD-A082 821 GENERAL MOTORS CORP INDIANAPOLIS IND DETROIT DIESEL --ETC F/G 21/5
HIGH BYPASS TURBOFAN COMPONENT DEVELOPMENT. PHASE II. FAN DETAI--ETC(U)
DEC 79 D C CHAPMAN F33615-78-C-2014
UNCLASSIFIED DDA-EDR-10026 AFAPL-TR-79-2103 NL

1 OF 1
AD A
082821

END
DATE
FILMED
5-80
DTIC

AFAPL-TR-79-2103

LEVEL II

ADA082821

HIGH BYPASS TURBOFAN COMPONENT DEVELOPMENT

Phase II—Fan Detail Design

D. C. Chapman

Detroit Diesel Allison
Division of General Motors Corporation
P. O. Box 894
Indianapolis, Indiana 46206

December 1979

TECHNICAL REPORT AFAPL-TR-2103

Final Report for December 1978 to October 1979

Air Force Aero Propulsion Laboratory
Air Force Wright Aeronautical Laboratories
Air Force Systems Command
Wright-Patterson Air Force Base, Ohio 45433

80 4 4 052

NOTICE

When Government drawings, specifications, or other data are used for any purpose other than in connection with a definitely related Government procurement operation, the United States Government thereby incurs no responsibility nor any obligation whatsoever; and the fact that the government may have formulated, furnished, or in any way supplied the said drawings, specifications, or other data, is not to be regarded by implication or otherwise as in any manner licensing the holder or any other person or corporation, or conveying any rights or permission to manufacture, use, or sell any patented invention that may in any way be related thereto.

This report has been reviewed by the Information Office (OI) and is releasable to the National Technical Information Service (NTIS). At NTIS, it will be available to the general public, including foreign nations.

This technical report has been reviewed and is approved for publication.

Larry W. Gill

LARRY W. GILL
Project Engineer

Erik W. Lindner

ERIK W. LINDNER
Tech Area Manager

FOR THE COMMANDER

Isak J. Gershon

ISAK J. GERSHON
Acting Branch Chief
Propulsion Branch
Turbine Engine Division

"If your address has changed, if you wish to be removed from our mailing list, or if the addressee is no longer employed by your organization please notify AFAPL/TBP *,W-PAFB, OH 45433 to help us maintain a current mailing list".*

Copies of this report should not be returned unless return is required by security considerations, contractual obligations, or notice on a specific document.

SECURITY CLASSIFICATION OF THIS PAGE (When Data Entered)

(19) REPORT DOCUMENTATION PAGE

READ INSTRUCTIONS BEFORE COMPLETING FORM

1. REPORT NUMBER: (18) AFAPL-TR-79-2103
2. GOVT ACCESSION NO.:
3. RECIPIENT'S CATALOG NUMBER:

4. TITLE (and Subtitle): (6) HIGH BYPASS TURBOFAN Component DEVELOPMENT, PHASE II - FAN DETAIL DESIGN,

5. TYPE OF REPORT & PERIOD COVERED: (9) Final Report, Dec 1978–Oct 1979

6. PERFORMING ORG. REPORT NUMBER: (14) DDA-EDR-10026

7. AUTHOR(s): (10) D. C. Chapman

8. CONTRACT OR GRANT NUMBER(s): (15) F33615-78-C-2014

9. PERFORMING ORGANIZATION NAME AND ADDRESS: Detroit Diesel Allison, Division of General Motors Corporation, P.O. Box 894, Indianapolis, Indiana 46206

10. PROGRAM ELEMENT, PROJECT, TASK AREA & WORK UNIT NUMBERS: (16) (17) 3066-15-24

11. CONTROLLING OFFICE NAME AND ADDRESS: Air Force Aero Propulsion Laboratory, Air Force Wright Aeronautical Laboratories, Air Force Systems Command, Wright-Patterson Air Force Base, Ohio 45433

12. REPORT DATE: (11) December 1979

13. NUMBER OF PAGES: 68

14. MONITORING AGENCY NAME & ADDRESS (if different from Controlling Office): (12) 69

15. SECURITY CLASS. (of this report): Unclassified

15a. DECLASSIFICATION/DOWNGRADING SCHEDULE

16. DISTRIBUTION STATEMENT (of this Report)

Approved for Public Release; Distribution Unlimited

17. DISTRIBUTION STATEMENT (of the abstract entered in Block 20, if different from Report)

18. SUPPLEMENTARY NOTES

Reference report - Phase I: AFAPL-TR-79-2034, High Bypass Turbofan Component Development, Phase I--Preliminary Design and Life Cycle Cost Analysis of Candidate Engines, D. C. Chapman and W. A. Redmond

19. KEY WORDS (Continue on reverse side if necessary and identify by block number)

Turbofan Engine, Trainer Enginer, Fan, Small Fan

20. ABSTRACT (Continue on reverse side if necessary and identify by block number)

The objective of this program is to develop an advanced, small, high bypass turbofan component applicable to an advanced, fuel-efficient engine for a new Air Force primary trainer aircraft. The program consists of two phases. Phase I consisted of the preliminary design and life cycle cost analysis of candidate engines. This report documents Phase II which was the detail design of the selected fan configuration. Primary design point of the fan is 1.8 pressure ratio at 55.9 lbm/sec flow. At a lower speed, the fan will produce 1.65 (cont)

DD FORM 1473, 1 JAN 73 — EDITION OF 1 NOV 65 IS OBSOLETE

Ø17 2ØØ

SECURITY CLASSIFICATION OF THIS PAGE (When Data Entered) pressure ratio at a flow compatible with the GMA500 advanced technology core engine. The resultant engine satisfies all requirements of the contract. The fan stage meets all requirements of Mil-E-5007D, including bird ingestion and predicted noise levels are below FAR Part 36 requirements.

Preface

This report was prepared by D. C. Chapman of Detroit Diesel Allison, Division of General Motors Corporation, Indianapolis, Indiana.

Design details of the fan stage designed in Phase II of Contract No. F33615-78-C-2014, High Bypass Turbofan Component Development, sponsored by the A.F. Aero Propulsion Laboratory are presented. The Air Force contract monitor was Capt. Larry Gill.

TABLE OF CONTENTS

LIST OF ILLUSTRATIONS

LIST OF TABLES

SUMMARY

An advanced technology fan stage adaptable to a small, high bypass turbofan engine for a future Air Force primary trainer has been designed. Primary design point is at 1.8 pressure ratio and 55.9 lb/sec flow. At a lower speed, this fan stage will produce a 1.65 pressure ratio at a flow compatible with the GMA500 core engine to form a high bypass engine meeting all requirements for the trainer application.

At the 1.8 pressure ratio design condition, the fan rotor operates at 1606 ft/sec tip speed with an inlet annulus specific flow of 42.3 $lbm/sec/ft^2$. The inlet hub/tip radius ratio is 0.40. The rotor has 20 blades of multiple circular arc airfoil sections with an aspect ratio of 1.64. Maximum thickness-to-chord ratio varies nonlinearly from 8.5% at hub to 2.5% at tip.

Forty-two vanes of multiple circular arc cross section are tilted rearward at the tip to increase blade to vane spacing for noise considerations. The vane aspect ratio is 2.32 and the maximum thickness-to-chord ratio varies from 6% at the hub to 8% at the tip.

The design meets all structural design requirements including steady and vibratory stresses, blade flutter, and bird ingestion. Substantial margins exist for blade and wheel permanent set at 122% speed and for burst at 130% speed. Adequate margins also exist for low cycle fatigue, considering 12,000 cycles to design speed with $K_t = 3$ at blade leading and trailing edges, $K_t = 1.4$ at blade crown, $K_t = 1.4$ in the wheel rim, and $K_t = 2.0$ in the wheel web. Allowable blade vibratory stress exceeds the required ± 15 ksi at resonance points and the required ± 5 ksi at nonresonance points.

The blading was also checked for torsional stall flutter and found to be satisfactory.

Bird ingestion requirements of Mil-E-5007D forced a slight thickening of the blade leading edge region in conjunction with a material change from titanium to stainless steel.

The predicted noise levels are substantially below FAR Part 36 levels at takeoff and approach. Furthermore, the ground idle noise levels are greatly reduced from those of the current trainer configuration.

SECTION I
INTRODUCTION

The current Air Force primary trainer (T37) fleet is approaching the end of its useful life, and a replacement aircraft will be needed. A fuel-efficient engine for the replacement aircraft must be developed. Advanced technology engines, such as the GMA500, suitable for the core of such a high bypass engine are being developed. Advanced technology fan stages in this size class are not available. To fill this void in technology, Detroit Diesel Allison (DDA), Division of General Motors Corporation, has conducted the High Bypass Turbofan Component Development Program for the United States Air Force Aero Propulsion Labratory, Wright-Patterson AFB, Ohio. The program consisted of two phases:

- Phase I--Preliminary Design and Life Cycle Cost Analysis of Candidate Engines
- Phase II--Detailed Design of the Fan stage chosen from Phase I

The Phase I studies were reported in Report No. AFAPL-TR-79-2034, High Bypass Turbofan Component Development, Phase I--Preliminary Design and Life Cycle Cost Analysis of Candidate Engines by D. C. Chapman and W. A. Redmond. This report documents the design of the fan stage completed in Phase II of the program.

Section II
DESIGN REQUIREMENTS

The core engine of choice in the Phase I selection process was the GMA500, an advanced technology turboshaft engine which was a winner in the United States Army Advanced Technology Demonstrator Engine (ATDE) Competition. DDA is currently under contract to complete 500 hours of running on the GMA500 engine starting early in CY 1979. The engine consists of a two-stage centrifugal compressor, foldback annular combustor, two-stage gasifier turbine, and two-stage power turbine.

In Phase I of this program, fans of 1.5, 1.65, 1.8, and 2.0 pressure ratio were matched with the GMA500 core engine to form candidate high bypass ratio engines for system life cycle cost analysis. The performance of all engines met or exceeded the requirements of this contract. Using representative aircraft characteristics, these engines, designated PD418, were applied to the mission requirements established by the Air Force. Both aircraft gross weight and system life cycle cost were minimized with a fan pressure ratio of 1.65, although the advantage of that pressure ratio over 1.5 and 1.8 pressure ratios was not great. DDA, therefore, recommended to the Air Force that the 1.65 pressure ratio fan be selected for detail design in Phase II of the program.

The Air Force identified a higher technology level with the 1.8 fan pressure ratio and because the Life Cycle Cost (LCC) penalty was small, selected that pressure ratio for Phase II. DDA preferred the 1.65 pressure ratio not only because of the LCC analysis but because the engine sea level static thrust level was approximately 7.5% greater than the engine with 1.8 fan pressure ratio. A mutually agreeable set of design conditions were established wherein the fan would be designed to achieve 1.65 pressure ratio at a flow compatible with the GMA500 core engine and also to achieve 1.8 pressure ratio at a higher flow and speed. The primary design point thus established is:

- Pressure ratio 1.8:1
- Corrected flow 55.86 lbm/sec
- Efficiency 85%

The secondary design point, which matches the GMA500 core engine requirement at 25,000 ft, 0.5 Mach number is:

- Pressure ratio 1.65:1
- Corrected flow 52.8 lbm/sec
- Efficiency 87%

Structurally, the fan should meet the requirements of Mil-E-5007D, including bird ingestion capability. Furthermore, the fan noise levels should be within the limits of FAR Part 36 at both takeoff and approach. An unofficial goal was to achieve a substantial reduction in noise at ground idle compared to the existing primary trainer.

SECTION III
AERODYNAMIC DESIGN

The aerodynamic design is presented at the 1.8 fan pressure ratio operating condition. Flow-path and vector diagram details are followed by rotor and stator blading information.

FLOW-PATH AND VECTOR DIAGRAMS

The design parameters for the small high bypass fan are:

• Stage pressure ratio	1.8:1
• Corrected flow rate, lbm/sec	55.86
• Adiabatic efficiency, %	85.2
• Rotor inlet hub/tip radius ratio	0.40
• Corrected tip speed, ft/sec	1606
• Corrected speed, rpm	21685
• Mechanical speed, rpm	20223
• Corrected specific flow rate, $lbm/sec/ft^2$	42.28

The velocity diagrams of the fan were obtained using the DDA Axial Compressor Design System. A description of the design system is given in Appendix A.

The fan was designed at an altitude cruise condition of 25,000 ft at 0.5 Mach number. This point represents the maximum mechanical speed achieved by the fan in a representative trainer mission.

A schematic of the fan flow-path is shown in Figure 1. The fan has a constant tip diameter of 16.974 in. and a rotor inlet hub-to-tip radius ratio of 0.40. The rotor hub ramp angle is 31.25 deg. The number of rotor airfoils is 20 while the stator has 42 vanes. The number of vanes and the vane-blade spacing were consequences of acoustical considerations.

The average value of the blade inlet absolute Mach number is 0.617. The blade inlet relative Mach numbers are supersonic for the outer 75% of the span. The exit relative Mach numbers are all subsonic (Figure 2). The average vane exit Mach number is 0.465. The inlet and exit Mach number profiles for the vane are shown in Figure 3.

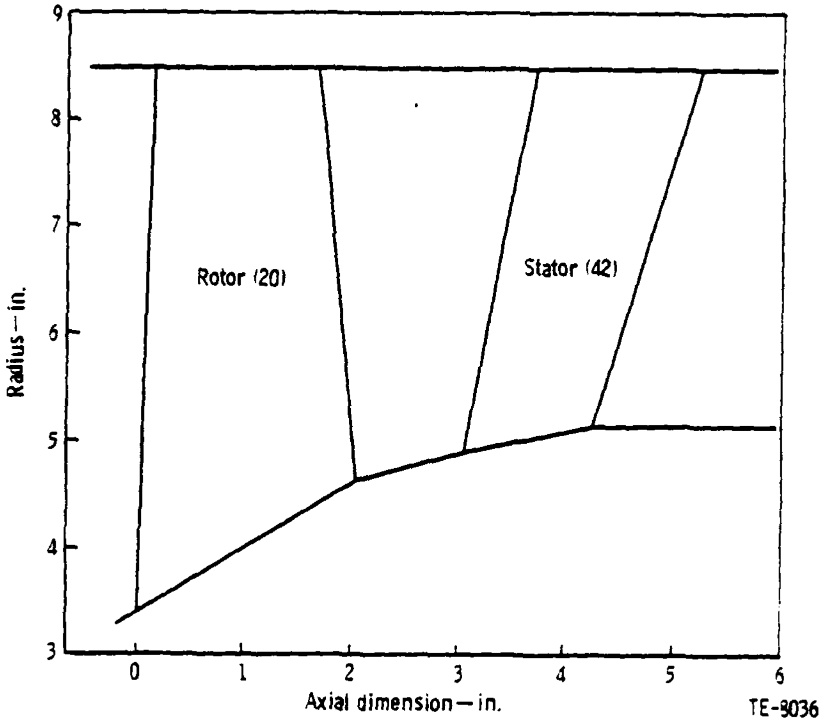

Figure 1. Schematic of fan flow path.

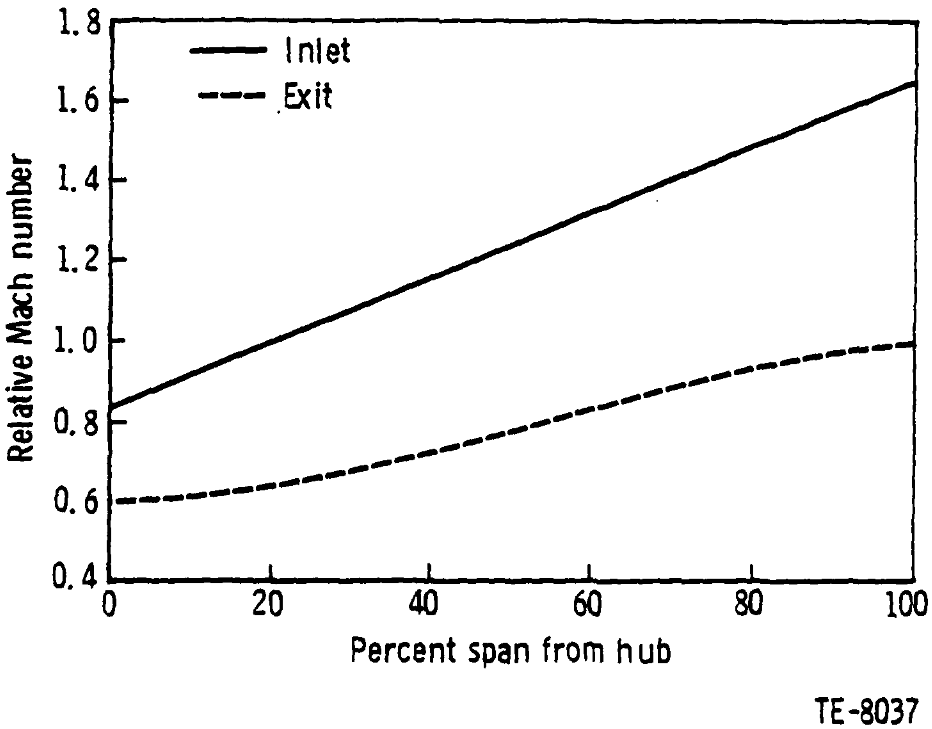

Figure 2. Blade Mach numbers.

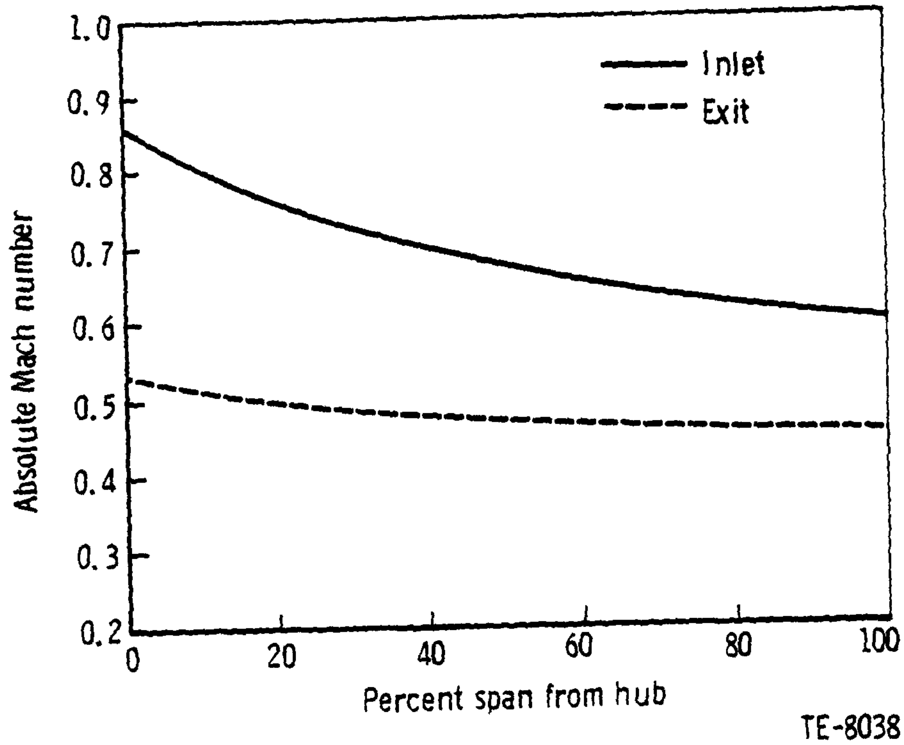

Figure 3. Vane Mach numbers.

The predicted blade and vane total pressure loss coefficients are illustrated in Figure 4. The resulting average efficiencies are 88.4% for the blade and 85.2% for the stage. The spanwise distribution of the design point loadings (diffusion factors) are shown in Figure 5. They are moderately high but the estimated surge margin for the fan is 18.6%. This surge margin estimate is based on a correlation of blade aspect ratio, relative Mach number, and tip loading at surge for various single stage compressors (Figure 6).

Figure 7 shows the blade inlet and exit relative air angles while Figure 8 is a plot of vane turning angles. The exit air angle from the vane is designed to be 0.0 degrees (axial).

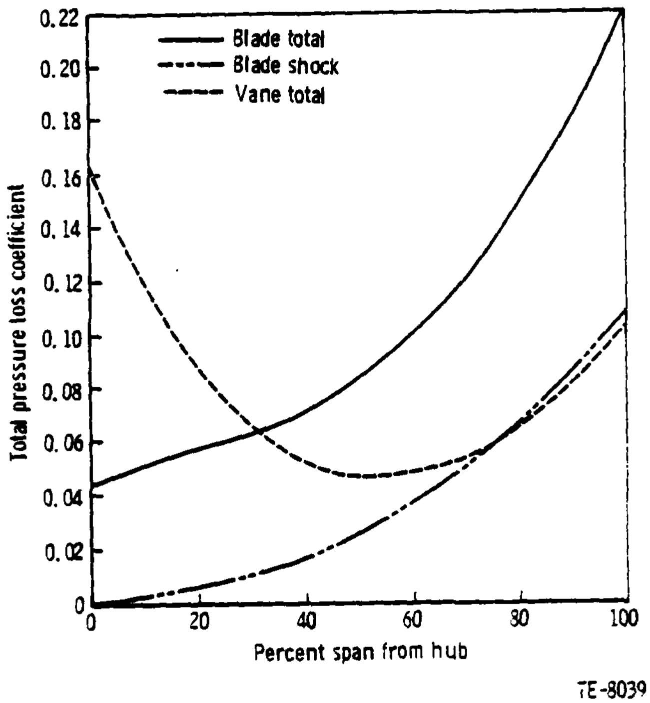

Figure 4. Radial distribution of total pressure loss coefficient.

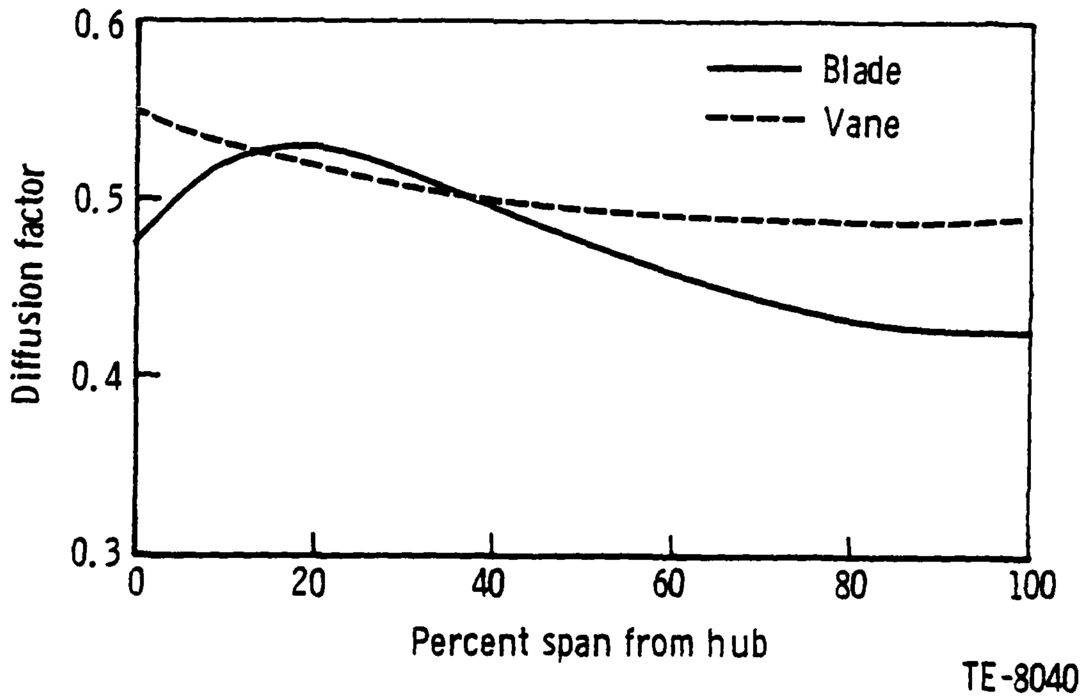

Figure 5. Blade and vane loading distributions.

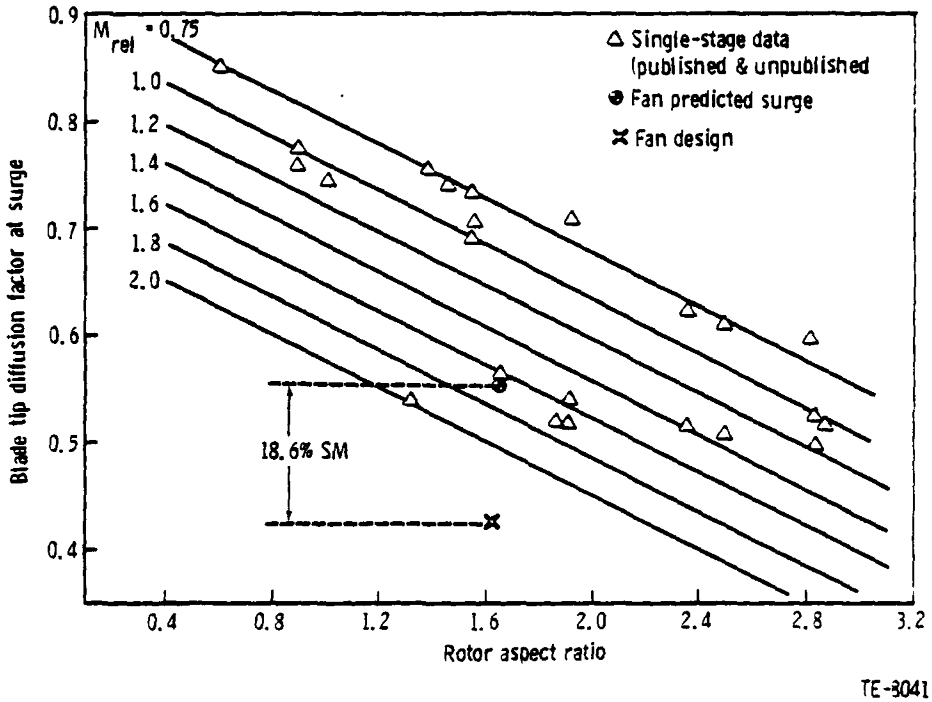

Figure 6. Single stage surge margin correlation.

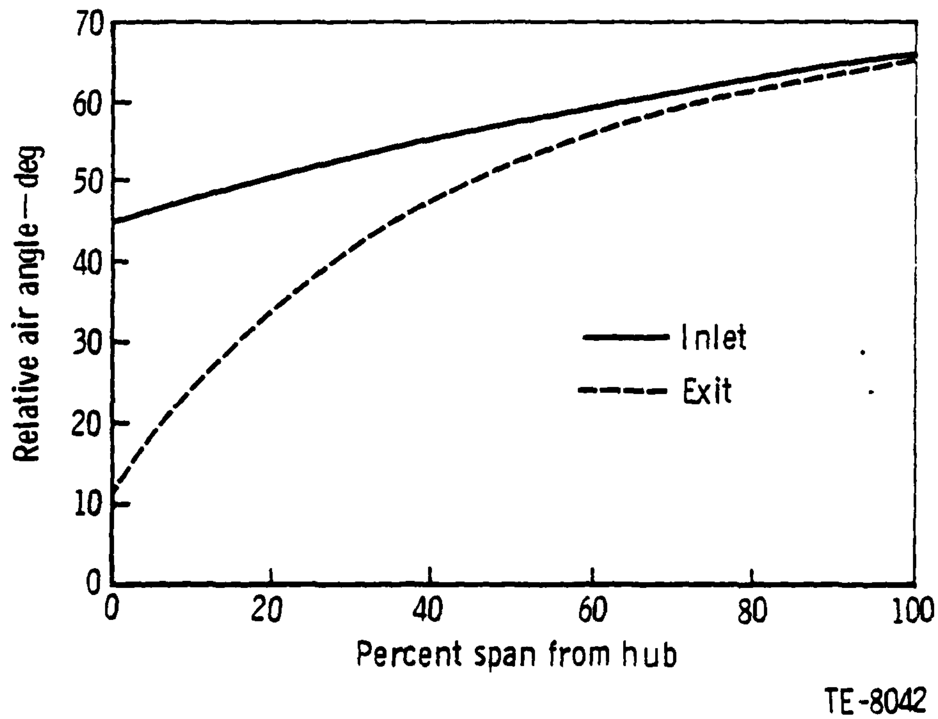

Figure 7. Blade air angles.

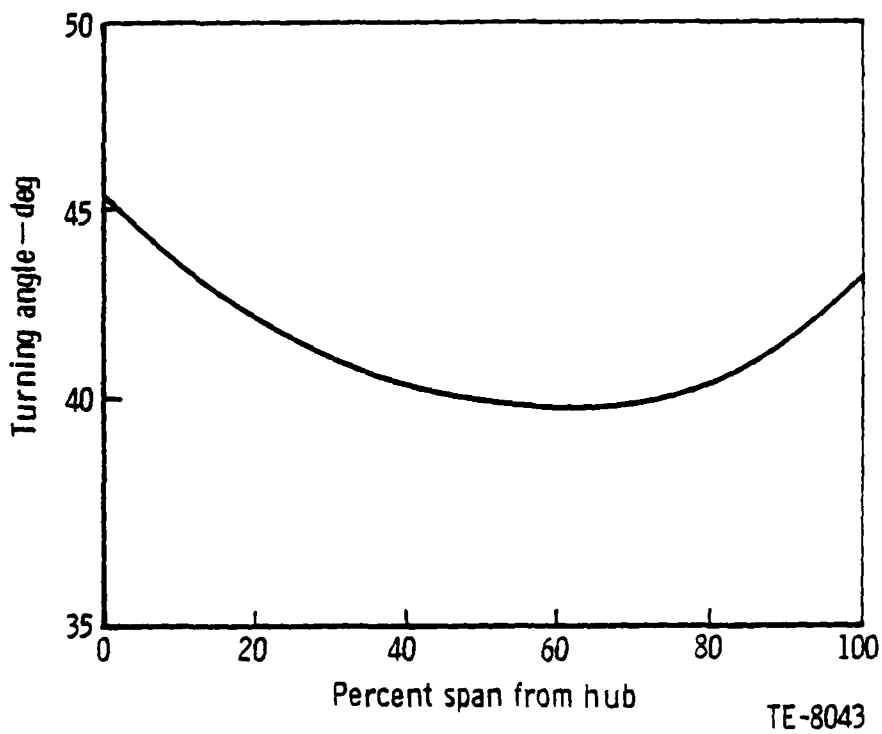

Figure 8. Vane turning angles.

The design point vector diagrams, calculated along streamlines, are tabulated for the blade and vane leading and trailing edge stations in Appendix B.

BLADE DESIGN

There are 20 blades with an aspect ratio of 1.64 (based on average span and true mean chord). The blade consists of multiple circular arc (MCA) airfoil sections designed on conical surfaces approximating streamlines of revolution. An MCA airfoil is shown schematically in Figure 9. It is made up of two circular arcs which define three metal angles: inlet (β_1*), exit (β_2*), and inflection (β_1*). A metal angle is the angle between the axial direction and the mean camber line at a specified location. A blade section is designed by adjusting the metal angles to satisfy incidence, deviation, and starting

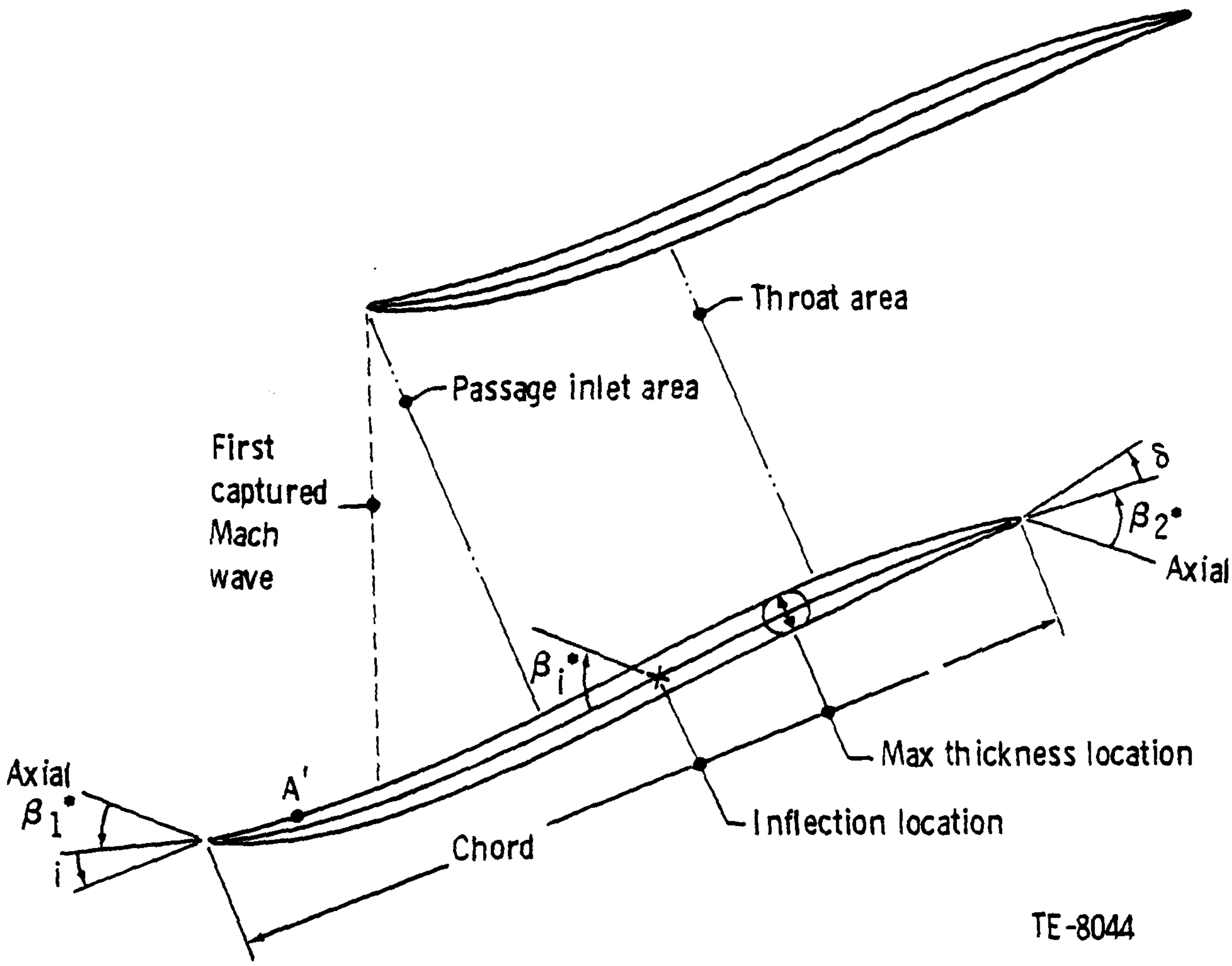

Figure 9. MCA airfoil definitions.

margin criteria. In the outer portion of the fan blade, where the inlet relative Mach number is supersonic, the airfoils were shaped to minimize shock loss. In the subsonic region of the blade, the airfoil shape transitions from the first supersonic section down to a near double-circular arc airfoil section at the hub.

A low aspect ratio, and, therefore, a long average chord, was selected to meet flutter criteria without the use of part-span shrouds. The spanwise chord taper was selected to satisfy the solidity requirements and also be viable from a weight and stress standpoint. The radial distributions of chord and solidity for the blade are shown in Figures 10 and 11, respectively. The maximum thickness to chord ratio (Figure 12) was set to avoid responsive resonant conditions and to maintain radial uniformity of blade mechanical properties. One of the mechanical considerations in the design was blade integrity with bird ingestion. The leading edge radius of the blade was set at 0.0125 in. from the hub to 60% span and then tapered to 0.010 in. at the tip. This maximized blade strength in the primary impact area while at the same time minimizing the efficiency penalty in the high inlet Mach number area at the blade tip from increased shock loss.

For the portion of the blade which has supersonic relative inlet Mach numbers, incidence was set on the suction surface at a point halfway between the leading edge and the emanation point of the first captured Mach wave (point A' of Figure 9). This incidence is the offset of the suction surface from a "free" streamline, which would exist if there were no blade forces, and it establishes the maximum flow the cascade can pass when the throat is not the limiting factor. The incidence value was set at 1.5 deg and is intended to account for leading edge blockage, suction surface boundary layer, and the bow shock wave. In the subsonic portion of the blade, the meanline incidence for each airfoil section was selected to locate the throat near the passage inlet.

Deviation angles were calculated using a modified form of the NACA 2-D rule for circular arc meanlines and then adding an empirical adjustment. The modification is a circulation correction based on the radius change of the streamline across the blade airfoil section.

The radial distributions of meanline incidence angle and deviation angle are shown in Figure 13. The resulting meanline blade angles are shown in Figure 14.

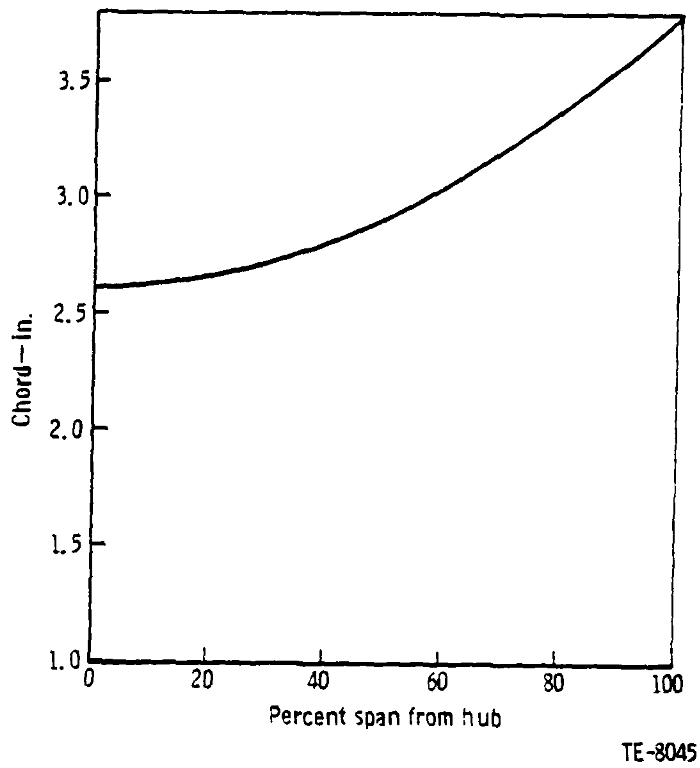

Figure 10. Blade chord.

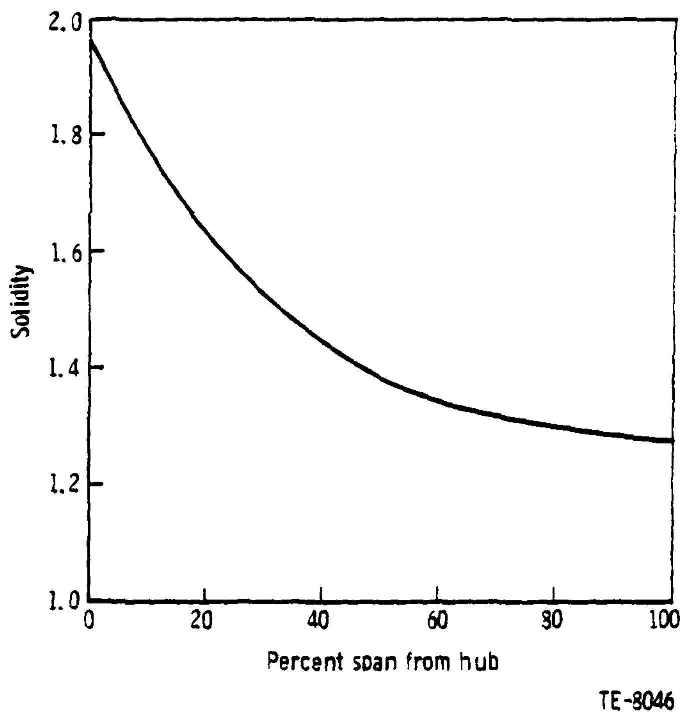

Figure 11. Blade solidity.

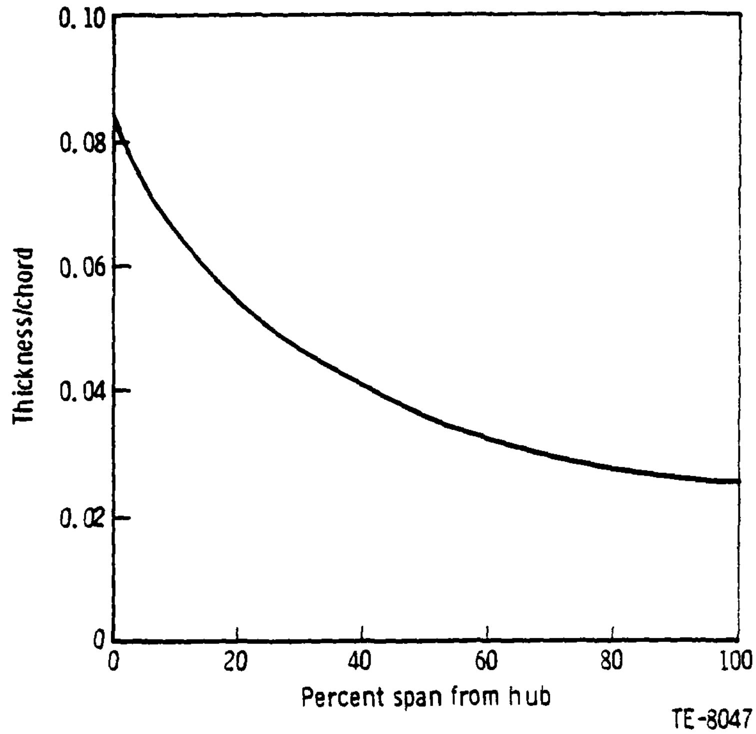

Figure 12. Blade maximum thickness/chord ratio.

The chordwise location of maximum thickness and circular arc inflection are shown in Figure 15. These were selected for two reasons: (1) to avoid accelerating suction surface curvatures ahead of the anticipated passage inlet shock wave location and (2) to set the passage inlet area and contour the airfoil passage between the passage inlet and the throat to minimize the velocity change through the passage. The design throat minimum critical area ratio (A/A* min) distribution for the supersonic airfoil sections is set to 1.03 for a normal shock total pressure loss applied at the passage entrance with a linear distribution of profile loss from the leading to trailing edge of the airfoil section. Streamtube contraction and the effect of radius change are accounted for.

Figure 16 shows the blade hub, mean, and tip conical airfoil sections in engine orientation. For manufacturing purposes, the airfoil sections were redefined on planes normal to the stacking line. The stack line is a radial line passing through the center of gravity of the hub conical section. The blade manufacturing coordinates are listed in Appendix C with definitions given in Figure C-1.

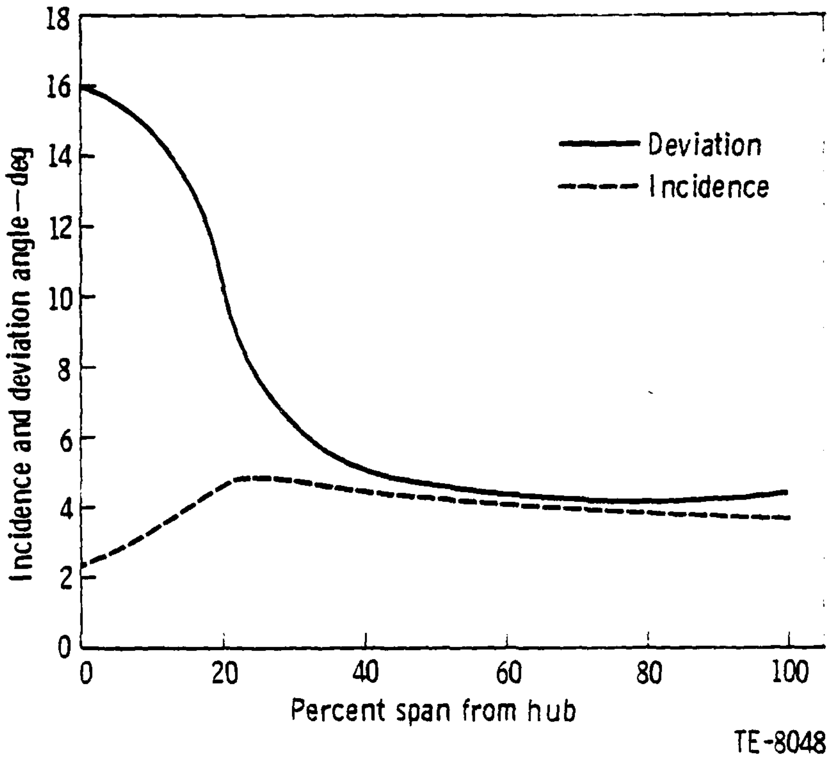

Figure 13. Blade incidence and deviation angles.

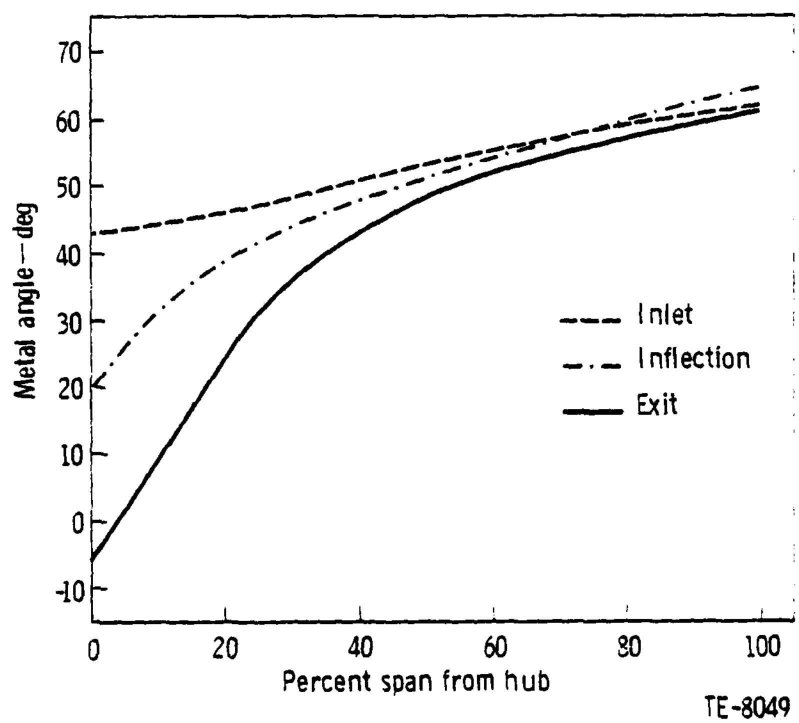

Figure 14. Blade metal angles.

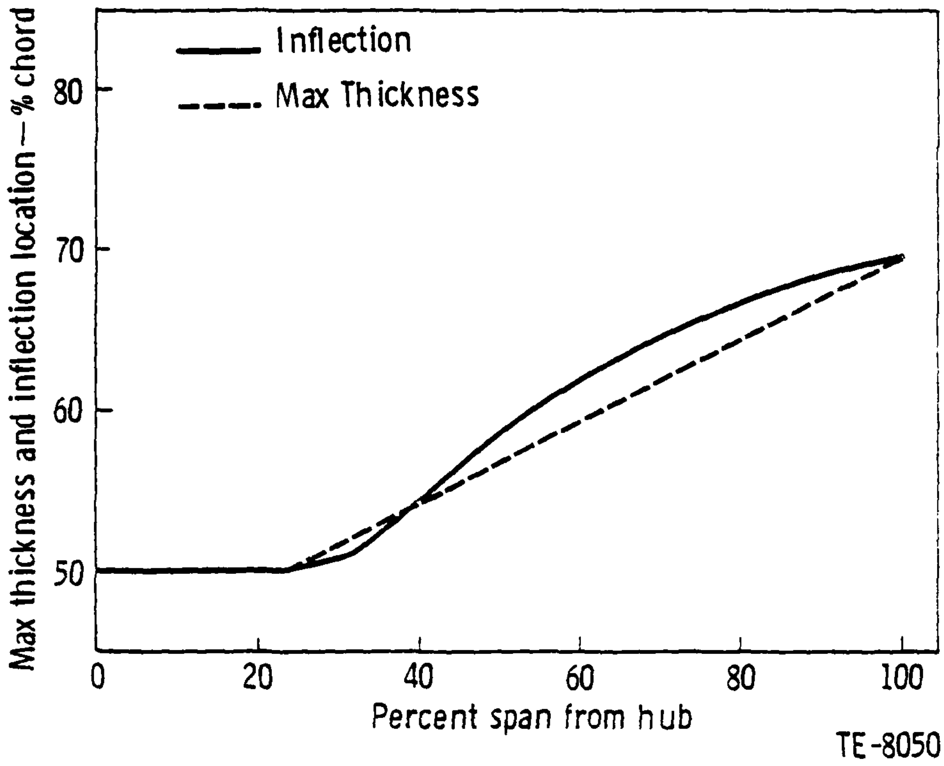

Figure 15. Blade maximum thickness and inflection locations.

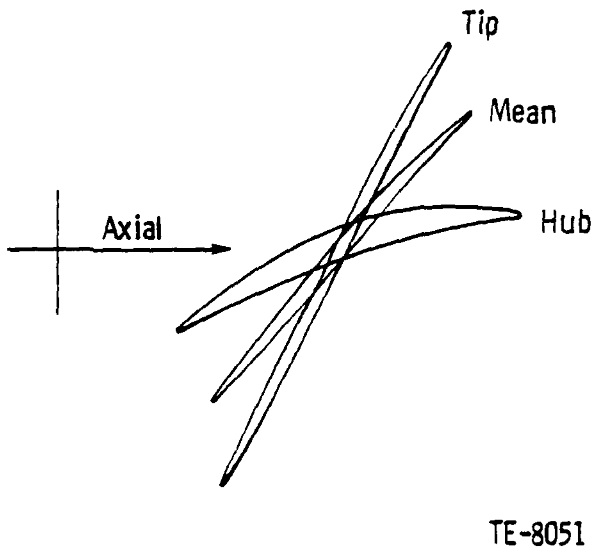

Figure 16. Blade conical airfoil sections.

VANE DESIGN

The vane is also made up of MCA airfoil sections. The vane axis is tilted rearward from radial at an angle of 13.5 deg. This gives a more desirable acoustic spacing between the blade and vane at the tip while minimizing hub length for bypass engine applications. There are 42 vanes with an aspect ratio of 2.32 and a solidity of 1.78 at the I.D. and 1.30 at the O.D. (Figure 17). The radial distribution of chord is shown in Figure 18. The maximum thickness to chord ratio varies linearly from 6% at the hub to 8% at the tip.

The incidence angles were selected to position the throat location at the vane passage inlet. The passage throat margins were based on minimum loss cascade data (Figure 19). Deviation angles were determined from the NACA 2-D rule with an empirical adjustment. The incidence and deviation angles for the vane are presented in Figure 20. Vane metal angles are shown in Figure 21. Vane hub, mean, and tip conical airfoil sections are illustrated in Figure 22.

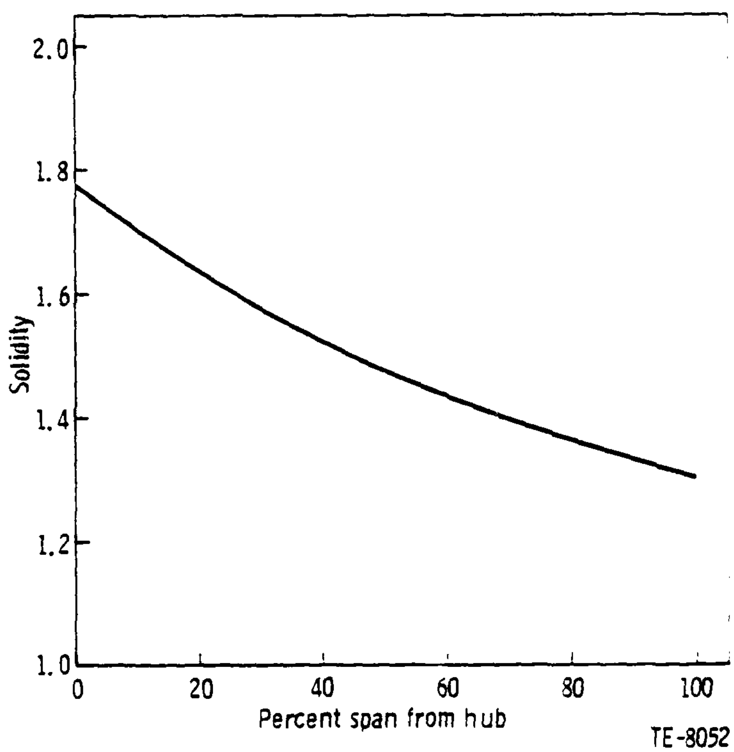

Figure 17. Vane solidity.

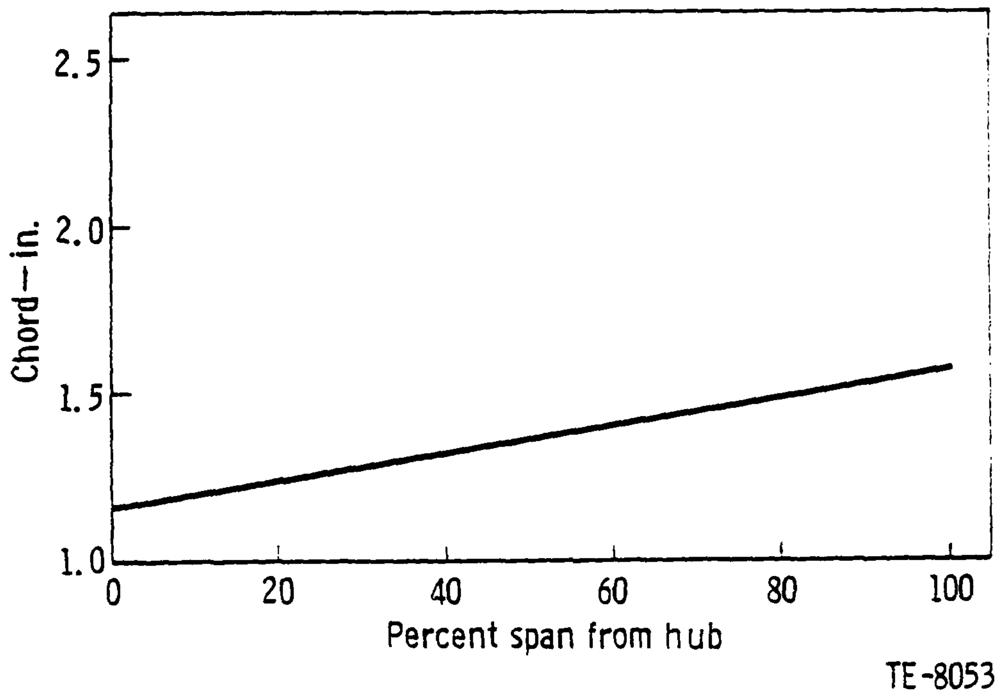

Figure 18. Vane chord.

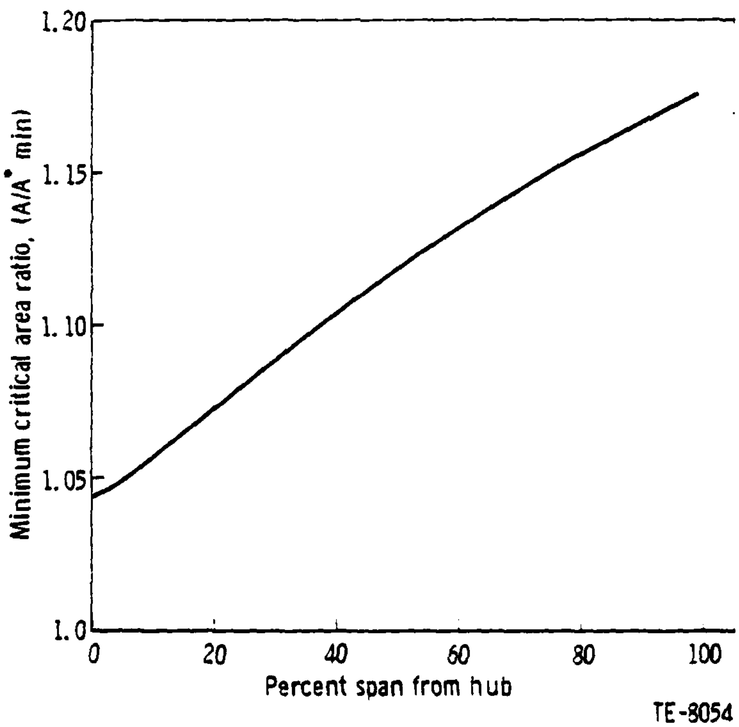

Figure 19. Vane passage throat minimum critical area ratio.

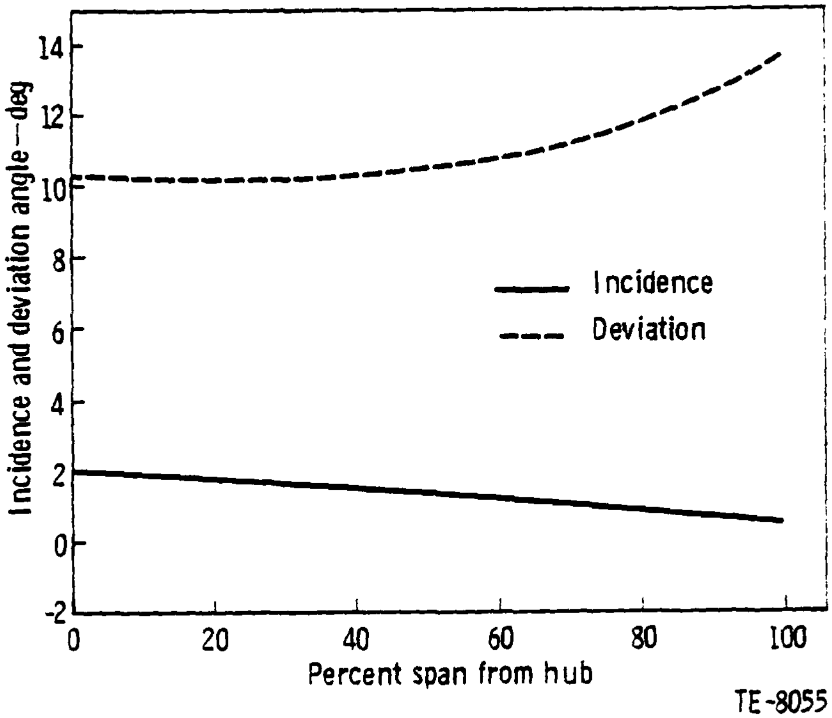

Figure 20. Vane incidence and deviation angles.

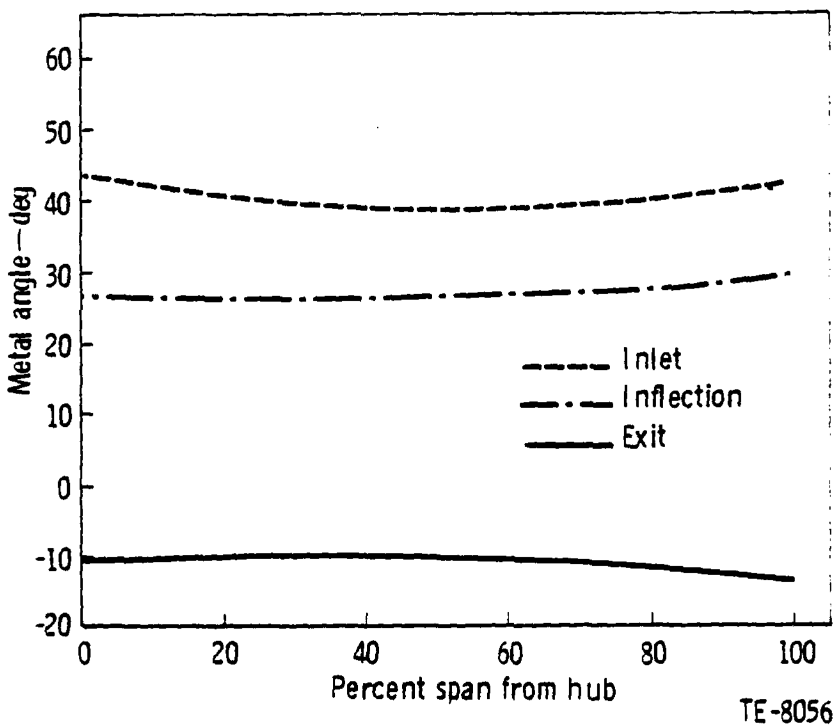

Figure 21. Vane metal angles.

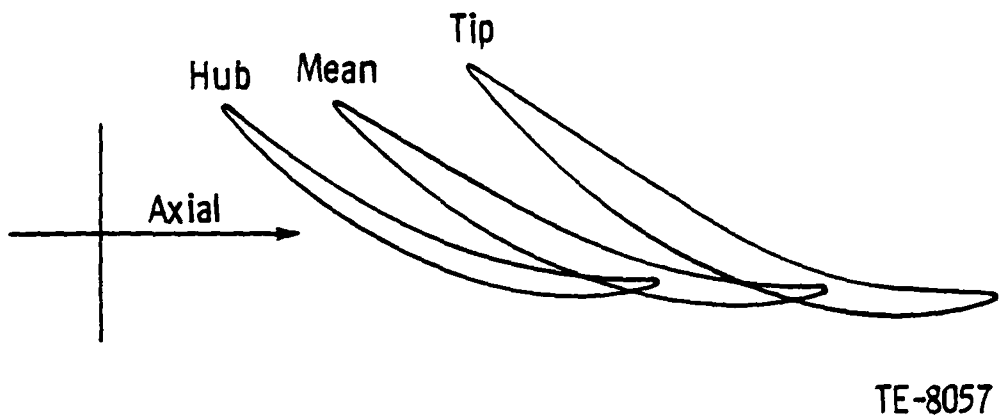

Figure 22. Vane conical airfoil sections.

The manufacturing coordinates for the vane are given in Appendix C with pertinent airfoil section definitions given on Figure C-2. The section coordinates were defined on planes normal to a stacking line. The stack line for the vane is on a radial line passing through the vane hub section c.g.

SECTION IV
STRUCTURAL ANALYSIS

Structural analysis of the fan rotor consisted of calculating airfoil and wheel steady-state stresses, airfoil vibrational characteristics, and bird ingestion capabilities. Satisfying all these requirements while retaining an aerodynamically acceptable configuration required numerous iterations on the design with changes in flow-path shape, spanwise chord and thickness distribution, and eventually a material change. The material change resulted from the inability to analytically satisfy bird ingestion requirements in an aerodynamically viable blade with titanium material. A stainless steel material (17-4 PH) was, therefore, substituted with consequent weight penalties. The final design meets or exceeds the requirements of Mil-E-5007D.

A titanium rotor (Ti-6Al-4V) design was near completion when the material change was deemed necessary. A satisfactory match-up of blade to wheel had not been obtained, and a valid hot-to-cold run was yet to be completed when the steel rotor analysis was started. Airfoil stresses reported here for the titanium rotor were determined with internal program boundary conditions for clamped hub, free tip. These automated constraints are not accurate for an integral blade-wheel rotor; preliminary blade/wheel match-up attempts indicated that airfoil crown stresses would be increased approximately 10 KSI over the reported results while leading edge and trailing edge stresses would be reduced.

The results of the analysis of the steel rotor are reported first. Titanium rotor results follow in a skeletonized format.

STEADY-STATE STRESSES

Design criteria for the rotor are given in Table 1. No steady-state blade stress will exceed 95% of the 0.2% yield strength of the material at 122% of design mechanical speed. High cycle fatigue requirements for the blade are a 15,000-psi allowable vibratory stress at resonance with a $K_t = 3.0$ at leading and trailing edges to allow for foreign object damage. Low cycle fatigue requirements for both wheel and blade are for greater than 12,000 start-stop cycles (zero-to-maximum stress) with a reliability of 0.9999. Finally, the wheel burst speed must exceed 130% of design speed.

TABLE I

Structural design criteria.

<u>Blade</u>

Permanent set	95% 0.2% yield @ 122% speed
Low cycle fatigue	12,000 start-stop cycles
High cycle fatigue	15 ksi allowable vibratory stress at resonance. FOD (K_t = 3.0) at leading and trailing edge

<u>Wheel</u>

Wheel burst	130% speed
Low cycle fatigue	12,000 start-stop cycles

Design point stress analyses were performed for the fan rotor at mechanical speeds of 20,223 and 18,950 rpm corresponding to 1.8 and 1.65 pressure ratios, respectively. The analysis is accomplished with finite element computer models which account for centrifugal loads, air loads, temperature effects, airfoil tilts, airfoil untwist, and wheel deflection. Airfoil bending stresses were minimized by tilting the airfoil in the direction of air loads.

Steel Rotor

Airfoil principal stress levels on both suction and pressure surfaces are shown for 1.8 and 1.65 pressure ratio design points in Figures 23 and 24, respectively. The maximum level of 110 ksi occurs near the airfoil hub on both suction and pressure surfaces at the higher pressure ratio and 100 ksi at the lower pressure ratio. The 110 ksi local principal stress on the blade surface compares with an average section stress of 61.5 ksi at design speed. To check the requirement for no damaging permanent set at 122% of design speed, it is

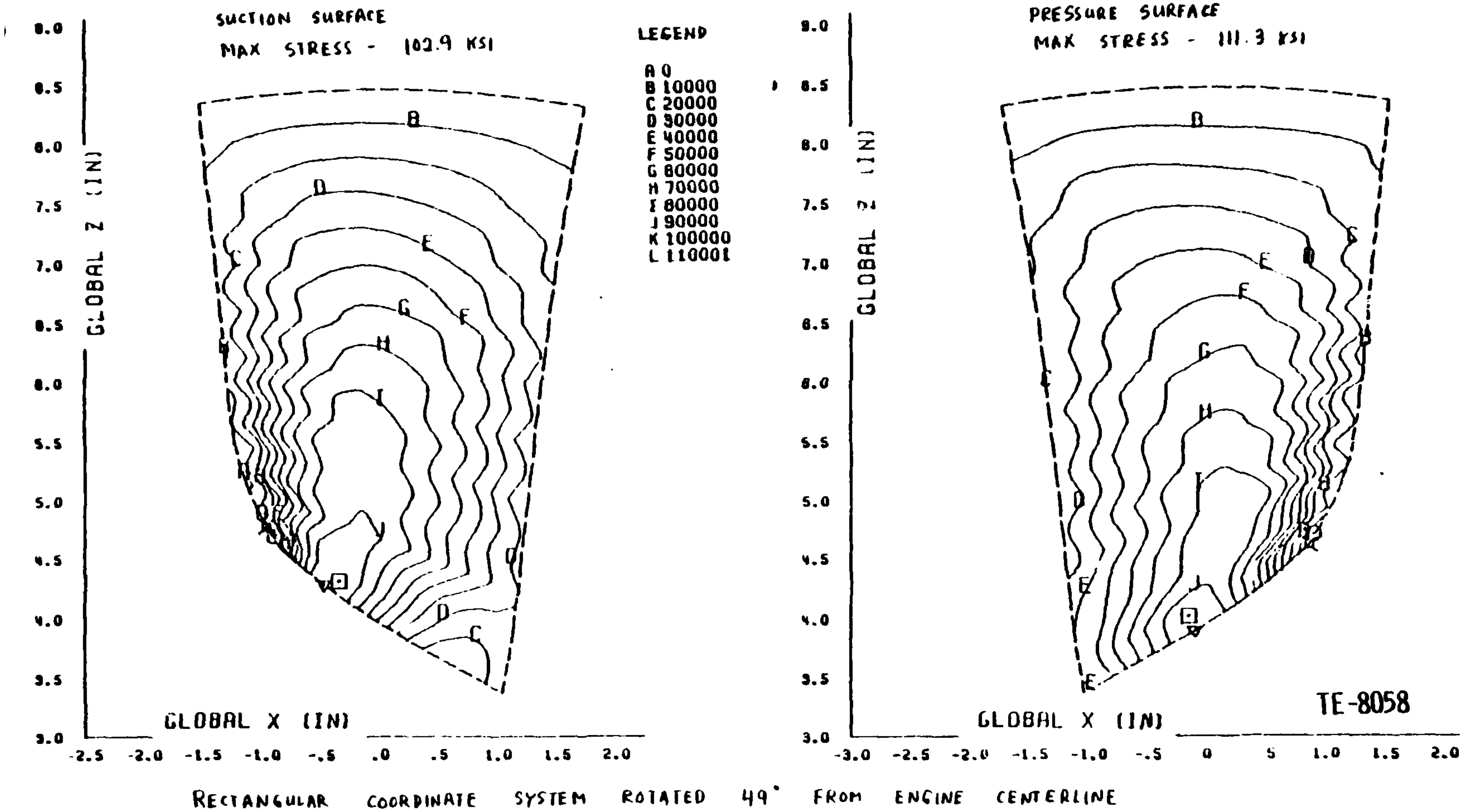

Figure 23. Principal blade stresses at 20,223 rpm.

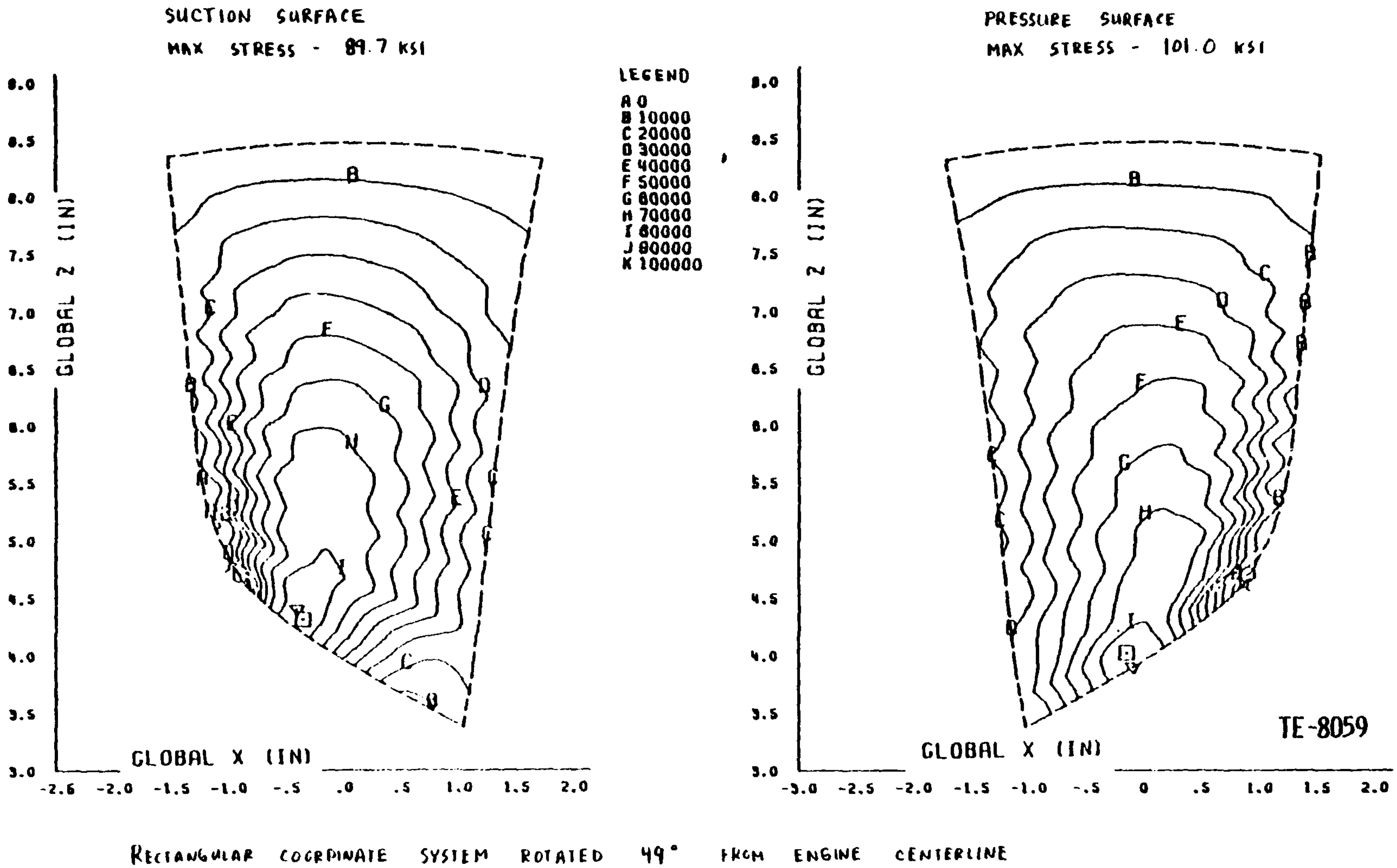

Figure 24. Principal blade stresses at 18,950 rpm.

TABLE 2

Blade stress summary.

Type of Failure	Criteria	Allowable Stress and Location, ksi	Calculated Section Average Stress 1.8 R_c, ksi	Calculated Section Average Stress 1.65 R_c, ksi
Permanent set	95% F_{T_y} @ 122% speed	137 crown	91.5	80.4
Burst	95% F_{T_u} @ 130% speed	151 crown	103.9	91.3
			Calculated Section Max Stress 1.8 R_c, ksi	**Calculated Section Max Stress 1.65 R_c, ksi**
Low cycle fatigue @ 100% speed	12,000 cycles K_t = 3	66 lead edge	46.3	39.2
	K_t = 3	66 trial edge	22.4	19.7
	K_t = 1.4	125 crown	110.0	100.3
High cycle fatigue	*±15 ksi vibratory @ resonance*	(Refer to Table 3)		
	±5 ksi vibratory @ nonresonance	±5 ksi crown (required)	±12.0 (allowable)	±14.4 (allowable)

necessary to scale the 61.5 ksi by the square of the speed ratio which gives an average stress level of 91.5 ksi at the overspeed condition. As shown in Table 2, this compares with an allowable stress of 137 ksi. Similarly, for a check of failure at 130% speed, the average stress scales to 104 ksi which compares with an allowable stress of 151 ksi.

Referring to the S-N diagram of Figure 25 at the 12,000-cycle requirement for low cycle fatigue, the airfoil leading and trailing edge allowable stresses are found to be 66 ksi based on a K_t = 3.0. The crown fillet allowable stress is 125 ksi based on a K_t = 1.4. Again, referring to Table 2, the calculated maximum principal stresses are well below these allowables.

The Goodman diagram of Figure 26 indicates that the 110 ksi maximum steady stress at the hub fillet, in conjunction with a fillet radius concentration factor of K_t = 1.4, provides a vibratory allowable stress at that location of ±12.0 ksi. Since this is not a potential resonance condition, a level of ±5 ksi would be considered satisfactory. The vibratory allowable stress at the hub fillet at the lower pressure ratio condition is ±14.4 ksi.

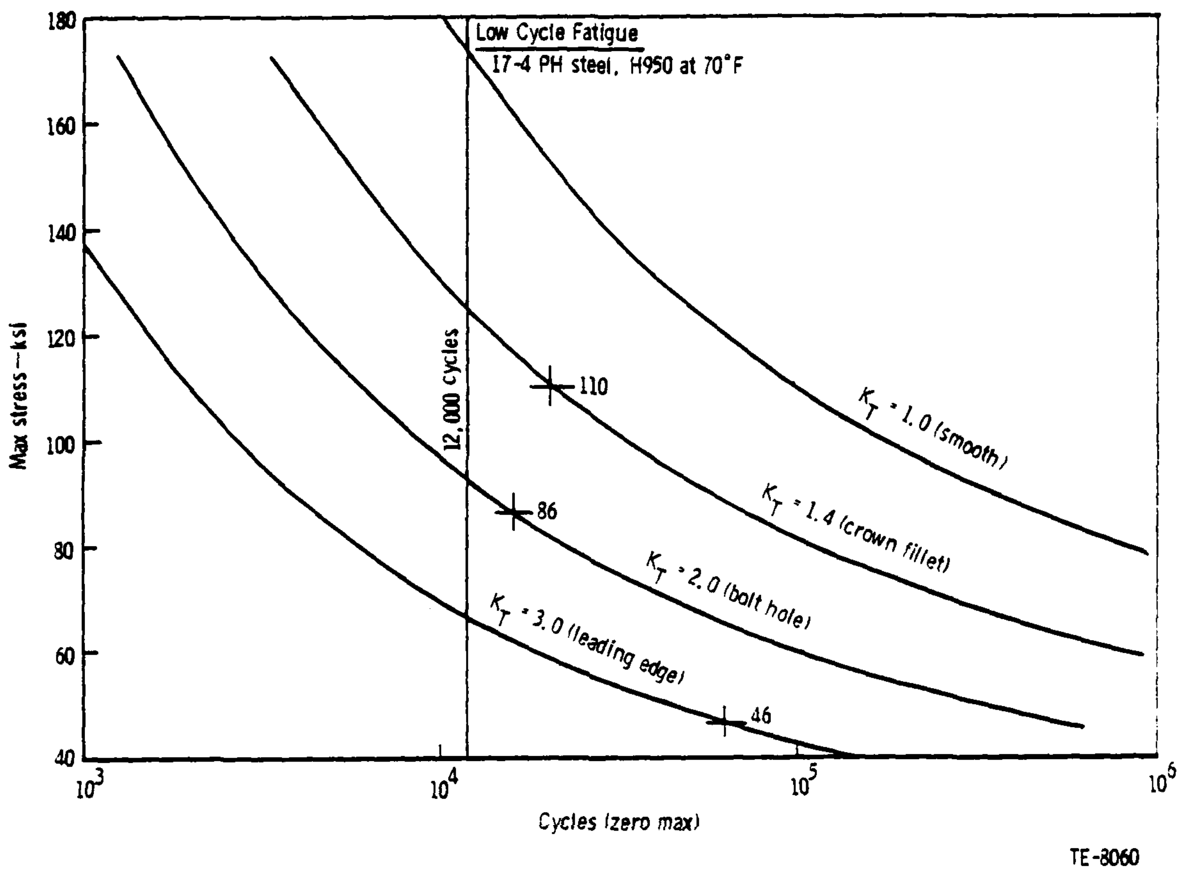

Figure 25. Fan blade and wheel S-N diagram.

Blade vibration analysis, to be discussed more fully later, indicates two potentially troublesome resonances in the operating envelope of the fan. These resonances are a second engine order-first bend mode coincidence at 11,800 rpm and a fourth engine order-first torsional mode coincidence at 18,800 rpm. Allowing a reasonable scatter of individual blade frequencies, the maximum static stresses at the maximum reasonance speed and at the critical vibratory stress points are given in Table 3. Entering the Goodman diagram of Figure 26 with those static stresses and the appropriate K_t values, the allowable vibratory stresses shown in Table 3 are defined. All these allowables exceed the goal of ±15 ksi vibratory allowable. It should also be noted that in the torsional mode, the dynamic stresses at location A and D are 50% and 85%, respectively, of the maximum dynamic stress which occurs at location B.

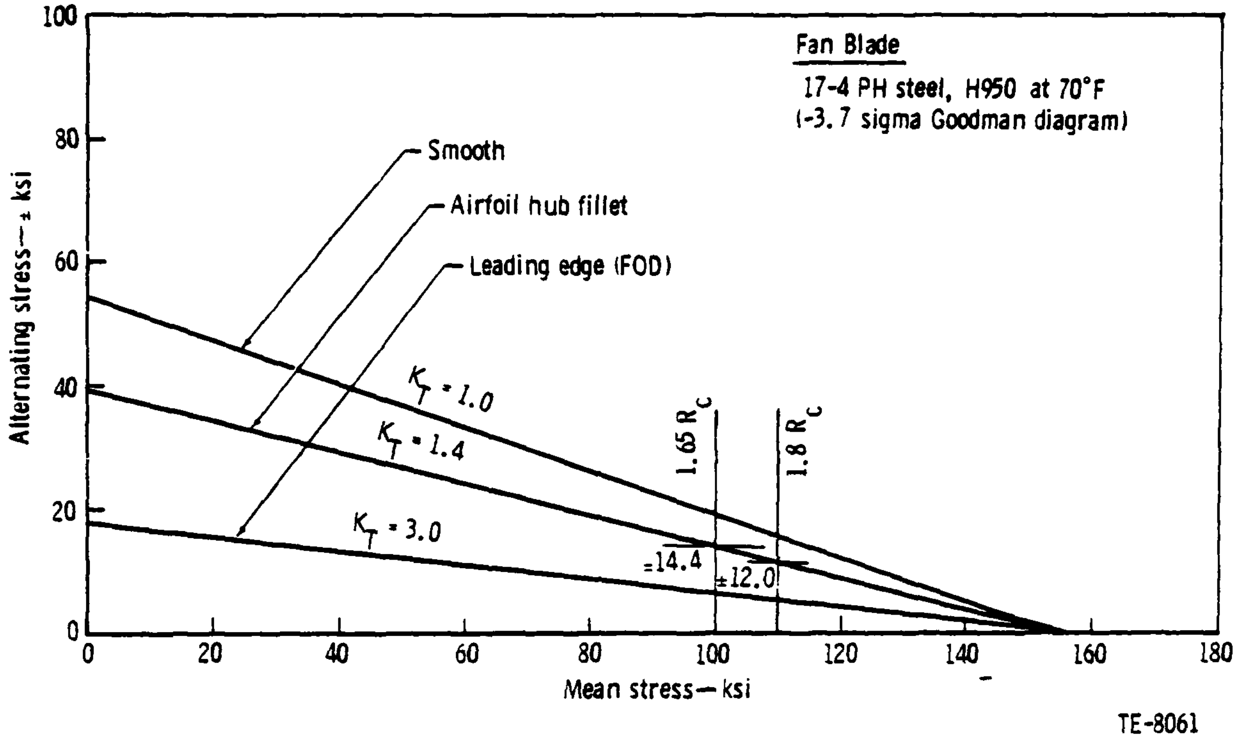

Figure 26. Fan blade Goodman diagram.

TABLE 3

Steel blade stress summary at maximum dynamic response.

High cycle fatigue allowables

17-4 PH steel

Cast properties

Mode	Location	Resonance Speed, rpm	Max Static Stress at Resonance, ksi	K_t	Allowable Vibratory Stress, ksi
First bend	A	11,800	35.0	1.4	±30.4
First torsion	A	18,800	95	1.4	±15.7
	D		23	3.0	±15.6
	B		8	3.0	±17.3

The airfoil, therefore, meets all static and dynamic stress criteria with appropriate K_t factors in cast 17-4 PH material.

Wheel equivalent stresses are shown in Figure 27. Referring to Table 4, a web equivalent stress of 128 ksi at 122% of design speed compared with an allowable yield stress of 137 ksi assures no detrimental permanent set at that condition. Checking wheel burst at 130% of design speed finds a calculated mean hoop stress of 102 ksi and a maximum web radial stress of 127 ksi at that condition which compares with an allowable stress level of 137 ksi. Actual wheel burst is assumed to occur when the mean hoop stress of the wheel reaches 95% of the ultimate strength of the material. The burst speed thus calculated is 163% of design speed or 33,000 rpm. In terms of low cycle fatigue, the calculated values of stress at rim, web, and bore are all well under the allowable stresses taken from the S-N diagram of Figure 25 at 12,000 cycles and the appropriate K_t factors.

TABLE 4

Steel wheel stress summary.

Type of Failure	Criteria	Allowable Stress and Location, ksi	Calculated stress, ksi	
			1.8 R_c	1.65 R_c
Permanent set	95% F_{T_y} @ 122% speed	137 web equiv.	128	112.4
Burst	86% F_{T_u} @ 130% speed	137 mean hoop	102	89.6
		137 web radial	127	111.5
Low cycle fatigue	12,000 cycles @ 100% speed			
	K_T = 1.4	125 rim hoop	56	49
	K_T = 2.0 (bolt hole)	92.5 web equiv.	86	75.5
	K_T = 1.0	174 bore hoop	92.8	81.5
	K_T = 3.0	67 balance holes	40	35

Therefore, the wheel also meets all design stress criteria in cast 17-4 PH material. The weight of the wheel and blades is approximately 16.3 lb.

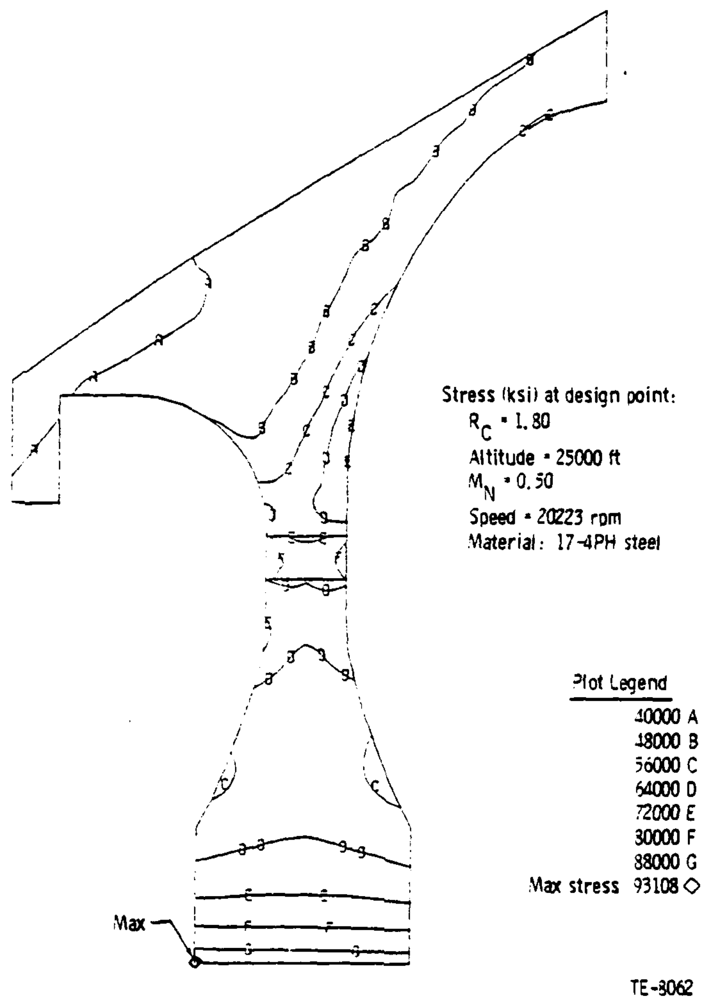

Figure 27. Wheel equivalent stresses.

Titanium Rotor

Blade stresses for the titanium rotor are summarized in Table 5 where allowable stresses for permanent set and burst are comfortably above calculated stresses. In the area of low cycle fatigue however, calculated stresses exceed the allowable at the leading edge and equal the allowable stress at the trailing edge for the 1.8 pressure ratio condition. These stresses are calculated for a rigidly clamped airfoil; including wheel rim flexibility would lower the edge stresses significantly.

TABLE 5

Blade stress summary.

Type of Failure	Criteria	Allowable Stress and Location, ksi	Calculated Section Average Stress	
			1.8 R_c, ksi	1.65 R_c, ksi
Permanent set	95% F_{T_y} @ 122% speed	92 crown	57.5	50.5
Burst	95% F_{T_u} @ 130% speed	99 crown	65.3	57.4
			Calculated Section Max Stress	
			1.8 R_c, ksi	1.65 R_c, ksi
Low cycle fatigue	12,000 cycles K_t = 3	39 lead edge	50	44
@ 100% speed	K_t = 3	39 trail edge	39	34.5
	K_t = 1.4	77 crown	53	47
High cycle fatigue	±15 ksi vibratory @ resonance		(Refer to Table 3)	
	±5 ksi vibratory @ nonresonance	±5 ksi crown	10.0	11.1
		(required)	(allowable)	(allowable)

Referring to Table 6, there are two resonances in the operating envelope of the titanium fan. The second engine order-first bend mode coincidence at 11,500 rpm produces a maximum vibratory response at location A where the static stress is 11.6 KSI. With a fillet radius concentration factor of 1.4 the allowable stress in cast titanium is ±17.5 KSI which exceeds the requirement of ±15 KSI. Similarly, the fourth engine order-first torsional mode coincidence at 18,800 rpm produces an acceptable allowable dynamic stress of ±18.4 KSI.

The titanium wheel stresses are summarized in Table 7 where the allowable stresses are seen to exceed calculated stresses by comfortable margins for all conditions. The calculated burst speed of the titanium wheel is 34,500 rpm or 171% of design speed.

The weight of the titanium wheel and blades is approximately 9.3 lbs, or approximately 7 lbs less than the steel rotor.

TABLE 6

Titanium blade stress summary at maximum dynamic response.

High cycle fatigue allowables

Titanium-6-4

Cast

Mode	Location	Resonance Speed, rpm	Max Static Stress at Resonance, ksi	K_t	Allowable Vibratory Stress, ksi
First bend	A	11,500	11.6	1.4	$\pm$17.5
First torsion	B	18,800	7.1	1.4	$\pm$18.4

TABLE 7

Titanium wheel stress summary.

Type of Failure	Criteria	Allowable Stress and Location, ksi	Calculated stress, ksi	
			1.8R_c	1.65 R_c
Permanent set	95% F_{T_y} @ 122% speed	92 web equiv.	79	69
Burst	86% F_{T_u} @ 130% speed	89 mean hoop	56.7	49.8
		89 web radial	79	69
Low cycle fatigue	12,000 cycles @ 100% speed			
	K_T = 1.4	77 rim hoop	32	28
	K_T = 2.0	56 web equiv.	53	47
	K_T = 1.0	102 bore hoop	52	46

VIBRATION ANALYSIS

Dynamic analyses of the airfoil, both vibration and flutter, are unaffected by the material change.

Frequencies, mode shapes, and relative dynamic stress distributions for all modes up through the vane passage frequency (42 EO) were calculated, using finite element techniques. The frequency versus speed interference diagram showing the first three modes is shown in Figure 28. The overall interference diagram is presented in Figure 29. Note that the first bending mode (1B) crosses 2 EO at relatively low speed (60%) such that the excitation levels due to inlet distortion will be low.

The relative dynamic stress distributions are determined to locate the maximum dynamic stress location for each mode to assess, in combination with the steady-state stress calculation, the allowable vibratory stress levels. Figures 30 and 31 show the relative radial dynamic stress distributions for the first two modes. These first two modes are given particular emphasis since the excitation force levels produced by the lower four engine orders are us-

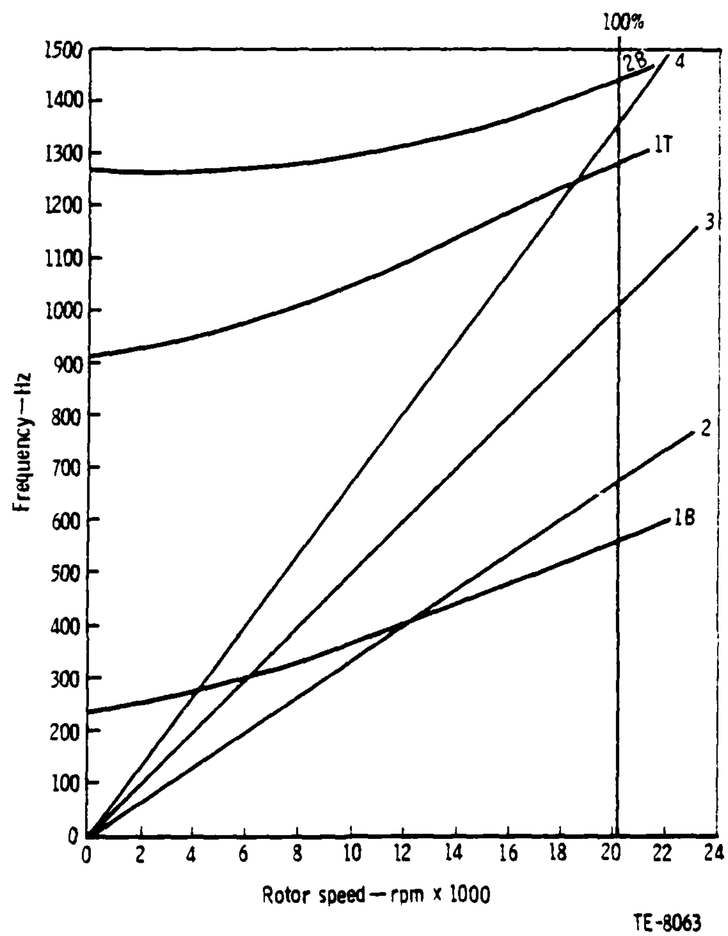

Figure 28. Frequency-speed interference diagram (first 3 modes).

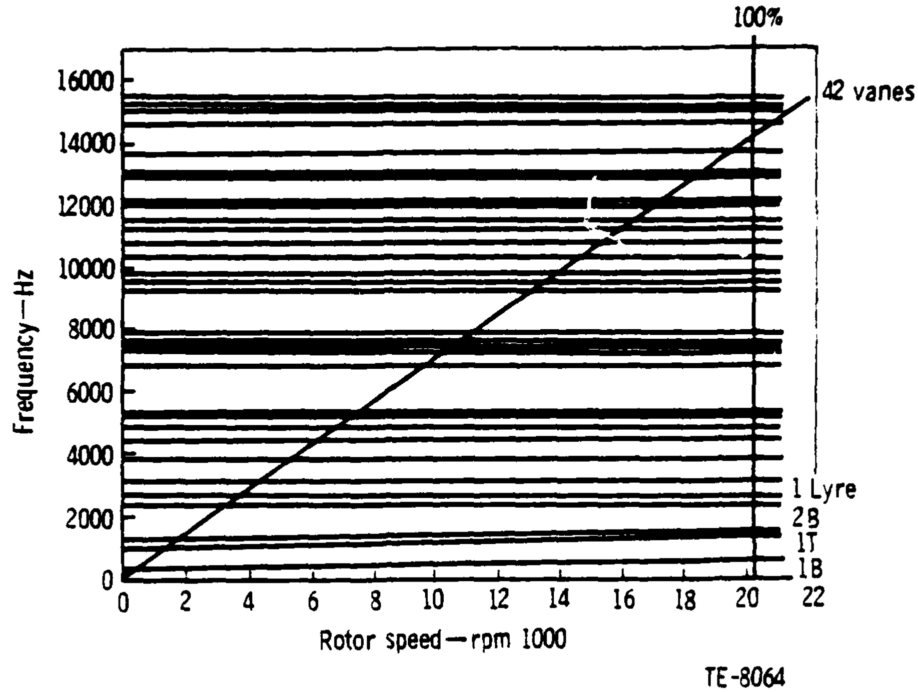

Figure 29. Frequency-speed interference diagram (first 32 modes).

ually higher than those generated by higher harmonics of rotor rotation. As previously discussed, the results of the allowable vibratory stress determination using the Goodman diagram, predicted steady-state stress at coincidence speed, and relative dynamic stress distributions satisfied the ±15 ksi vibratory stress criteria.

Blade response because of a coincidence of high modes with vane passage (42 EO) are expected to be very low because of the large axial distance (1.5 chord lengths) that the vane row is located aft of the blade row. This large spacing is a result of the noise design criteria.

FLUTTER ANALYSIS

The results of the torsional stall flutter analysis are shown in Figure 32. The predicted margin of safety is an adequate 4 deg of incidence angle above the estimated operating line. The calculated bending stall flutter reduced frequency parameter is well above the 0.25 criterion at 0.302. Similarily, the supersonic unstalled reduced torsional frequency parameter at 0.68 satisfies the 0.60 requirement.

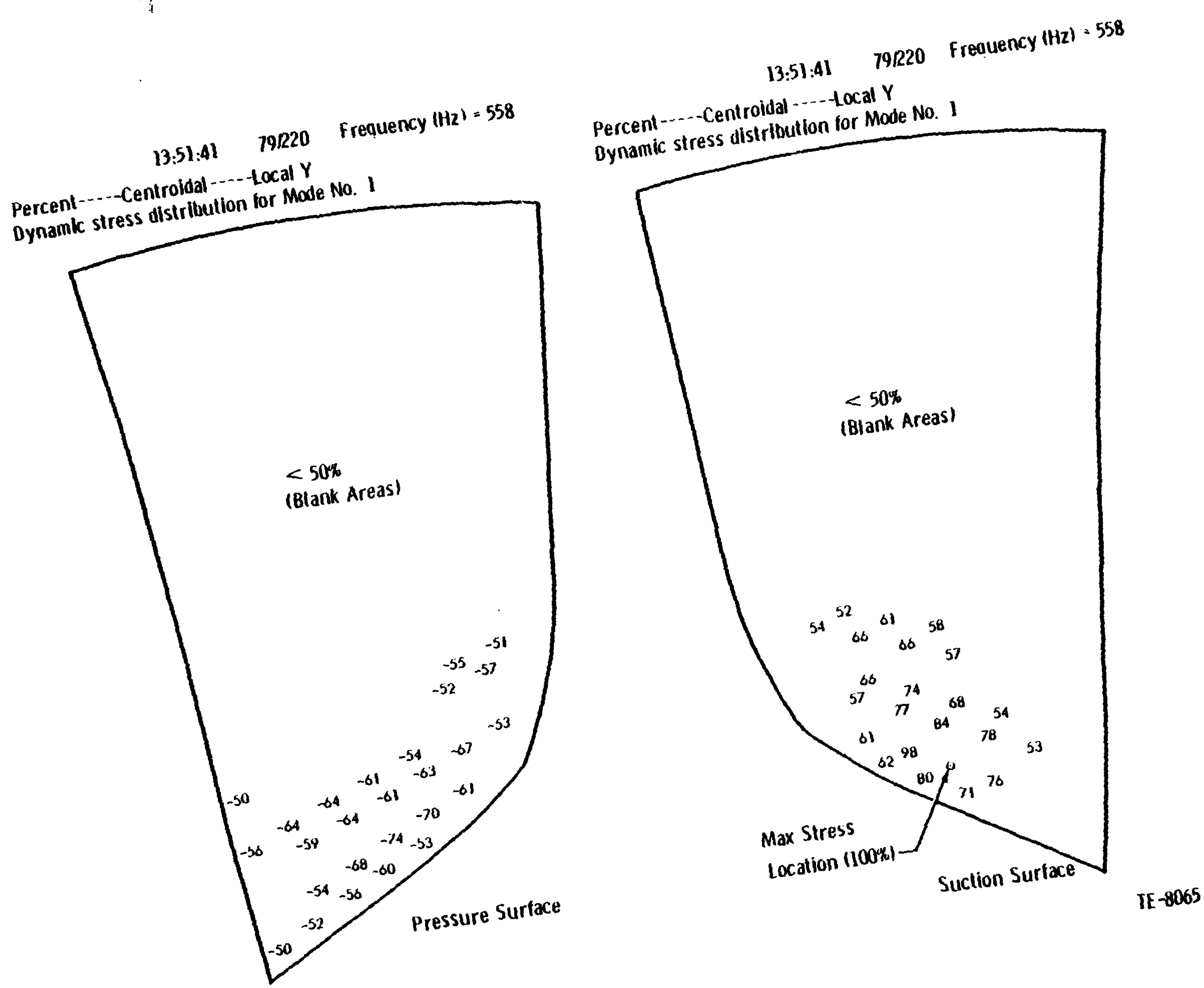

Figure 30. Relative dynamic stress distribution--1B mode at 20,223 rpm.

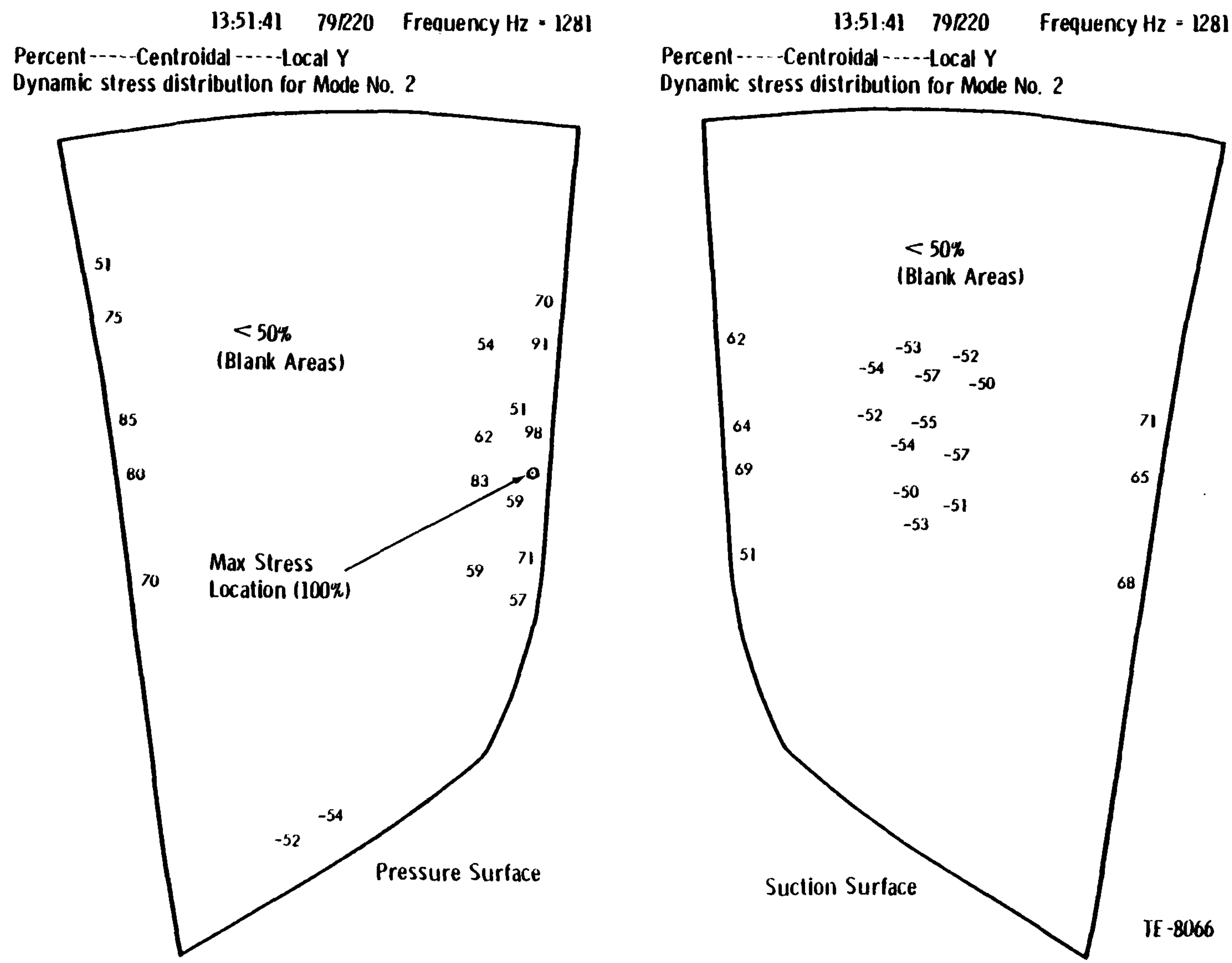

Figure 31. Relative dynamic stress distribution--1T mode at 20,223 rpm.

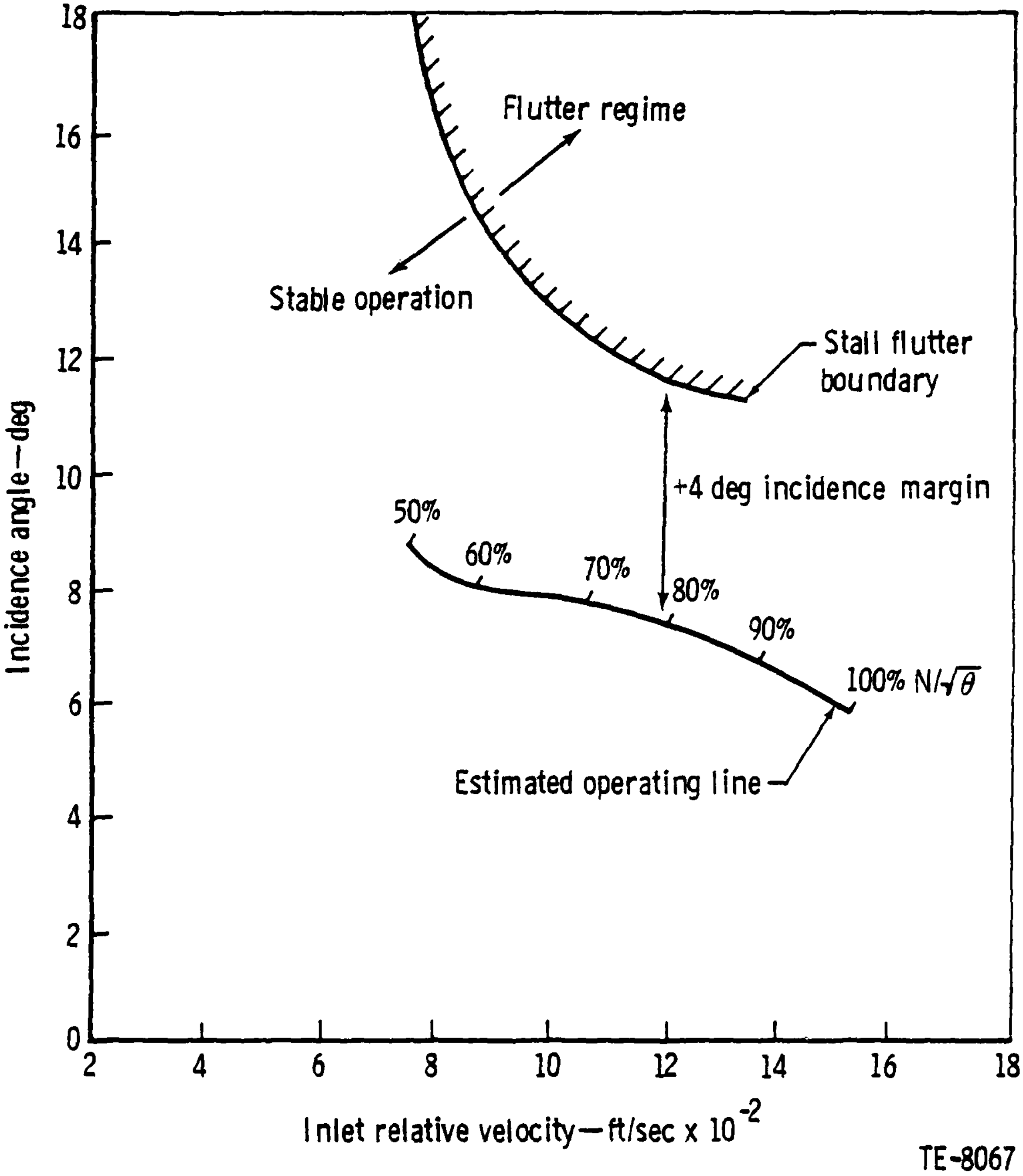

Figure 32. Stall torsional flutter analysis.

BIRD INGESTION ANALYSIS

The USAF requirements for bird ingestion are defined in Mil-E-5007D, paragraph 3.2.5.6.1. A summary of the specified bird sizes and engine conditions is given in Table 8. The small high bypass fan and typical trainer aircraft speeds corresponding to the Mil-E-5007D requirements are given in Table 9. In Table 9, the aircraft liftoff, climb, cruise, and descent speeds for the 1.80 pressure ratio fan are assumed to be the same as for the 1.65 pressure ratio fan application.

The annular inlet area of this fan is less than 200 $in.^2$ which sets the maximum bird size at two pounds (Ref. Mil-E-5007D par 3.2.5.6.1e). For bird impacts up to 2 lb, no failure shall result which will cause shutdown of the engine although some damage to engine parts may occur.

The failure mode considered here for bird ingestion is local impact damage in the leading edge region of the blade. The calculation of a local damage index, based on a Lycoming criterion approach (Ref. FAA-RD-77-55), has been incorporated into the DDA bird ingestion analysis. This approach relates significant bird slice, impact area, and airfoil parameters to a damage index value that corresponds to critical blade damage. An acceptable damage index level is determined by correlation with actual bird ingestion test data. Engine survivability for new blade designs at the critical ingestion conditions is then predicted with some confidence by use of the damage index calculation.

The shear-penetration damage index is expressed as

$$D_i = 0.273\ V_N \sqrt{\pi/4 \left(\frac{eD_B K_B}{h\tau_y}\right)}$$

where:

V_N = the normal component of impact velocity (ft/sec)

e = the bird density = 0.045 lb/in.^{3}

D_B = the bird diameter (in.)

h = the target mid-thickness (in.)

τ_y = the target material shear yield (psi)

K_B = the bird fragmentation parameter

TABLE 8

Mil-E-5007D bird ingestion requirements.

A. Birds weighing 2 to 4 ounces (a maximum of sixteen at a time) and birds weighing 2 pounds (one at a time) ingested at a bird velocity equal to the take-off flight speed, with the engine at maximum rated speed.

B. Birds weighing 2 to 4 ounces (a maximum of sixteen at a time) and birds weighing 2 pounds (one at a time) ingested at a bird velocity equal to the cruise flight speed with the engine at maximum continuous speed.

C. Birds weighing 2 to 4 ounces (a maximum of sixteen at a time) and birds weighing 2 pounds (one at a time) ingested at a bird velocity equal to the descent flight speed with the engine at an associated engine speed.

D. Birds weighing 4 pounds ingested at a bird velocity based on the most critical flight speed with the engine at maximum rated speed.

Note: Condition D does not apply since the trainer fan inlet is less than 200 in^2. A maximum of four birds weighing 2 to 4 ounces must be considered for the trainer fan.

TABLE 9

Fan and aircraft speeds for Mil-E-5007D conditions.

	Pressure ratio 1.65	Pressure ratio 1.80
Condition A		
Engine take-off fan speed (rpm)	17,303	18,465
Lift-off speed of typical aircraft (kts)	90	90
Climb speed of typical aircraft (kts)	198	198
Condition B		
Engine maximum continuous fan speed (rpm)	17,292	18,454
Cruise speed of typical aircraft (kts)	194	194
Condition C		
Engine descent fan speed (rpm)	10,377	11,074
Descent speed of typical aircraft (kts)	198	198
Condition D		
Engine cruise fan speed (rpm)	10,496	11,201
Cruise speed of typical aircraft (kts)	194	194

The values of D_B and K_B are defined by:

$$D_B = 3.48\ (\text{bird weight})^{0.33}$$

$$K_B = \begin{Bmatrix} 1.0 \\ 2.40-0.0054V_N \\ 2.5 \end{Bmatrix} \text{ for } \begin{Bmatrix} V_N \leq 260\text{ft/sec} \\ 260 < V_N < 400 \\ 400 \leq V_N \end{Bmatrix}$$

Figure 33 illustrates the region of leading edge impact.

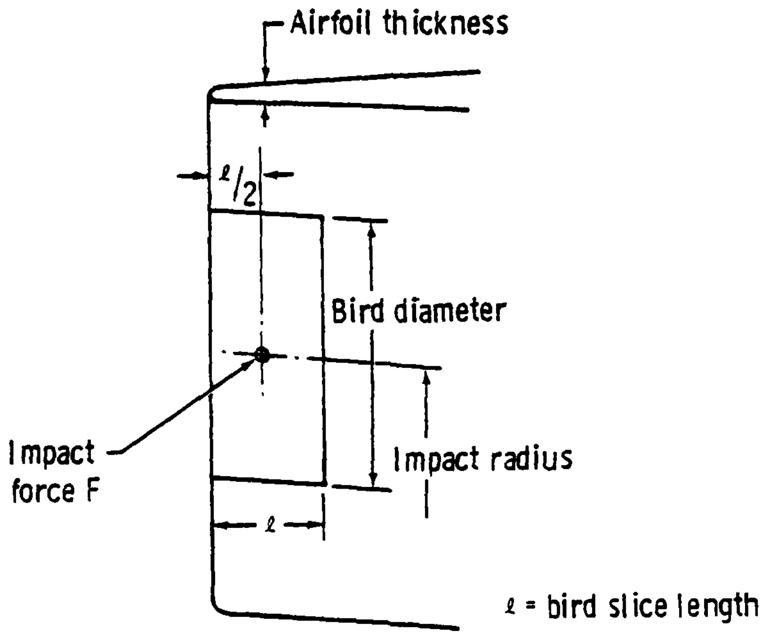

Figure 33. Bird impact area and blade thickness illustration.

The ballistic-limit velocity for total shear penetration is reached as the damage index approaches 1.0 and theoretically should cause maximum structural damage. In practice, the maximum allowable damage index must be determined by correlation with test.

The calculated damage index along the airfold span for a base-line titanium design at a 1.80 pressure ratio is shown in Figure 34. The maximum damage is predicted to occur at the outermost radial position permitted by the outer case and the 2-lb bird diameter. The maximum allowable damage index for shroudless airfoils is set at 0.40 which limits the expected damage to span-wise tears. A damage index greater than 0.40 could produce loss of airfoil section (for several blades at the 2-lb size) and would cause rotor unbalance that would require engine shut-down. On this basis, the base-line titanium design is judged unacceptable.

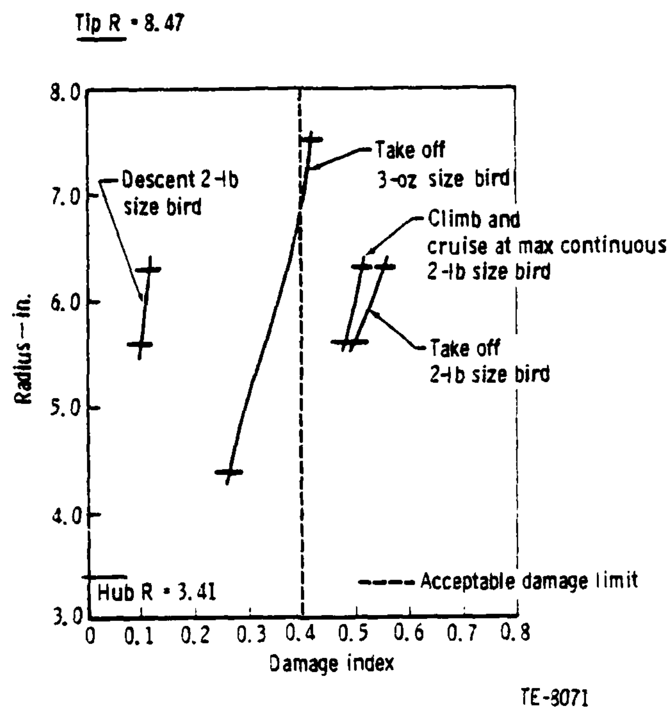

Figure 34. Bird ingestion damage index--titanium blade.

A design study was made to establish the damage index sensitivity to leading edge radius, thickness/chord, number of blades, etc, to identify an acceptable damage index domain for the titanium fan. A titanium airfoil with a 0.025-in. leading edge radius was found to have an acceptable index. However, the performance penalties associated with the required design changes were excessive. Thus, based on the bird ingestion requirements (which are particularly important for trainer engines), a switch to 17-4 PH stainless material was made. The advantage of the material is an increase in shear strength from 66.5 to 106 ksi.

The calculated damage index along the airfoil span for the steel design is shown in Figure 35. Again, the maximum index value of 0.39 is found to occur at the outermost radial position permitted by the outer case for the 2-lb size bird. The steel design (with a 0.0125 leading edge radius) thus satisfies the acceptable damage index limit of 0.40 for the this type of blading.

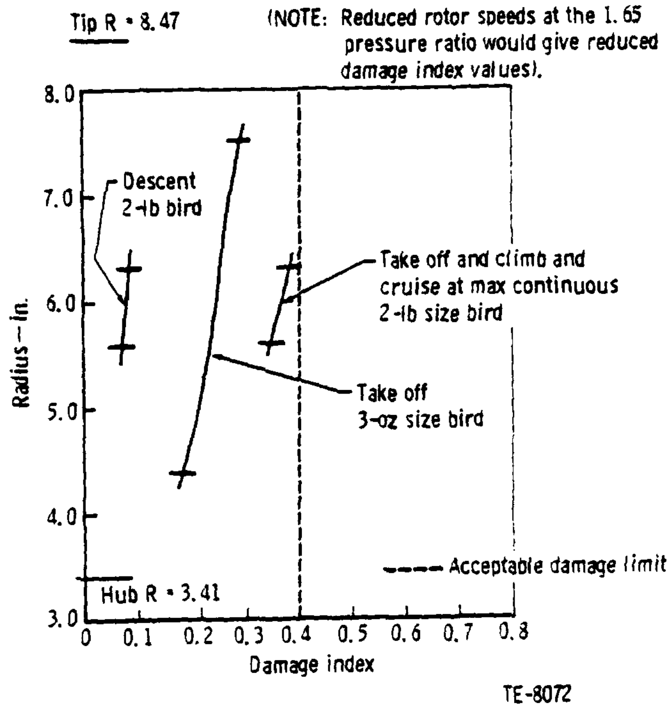

Figure 35. Bird ingestion damage index—steel blade.

Bird ingestion requirements have forced a change in leading edge thickness and material for this fan blade. The penalties are approximately one-half percentage point in stage efficiency and an increase in rotor weight from 9.25 to 16.25 lb. Any degradation in engine response during power transients have not been quantified.

SECTION V
NOISE PREDICTION

Noise goals for the high bypass turbofan powered undergraduate trainer are to be in compliance with Federal Air Regulation Part 36 requirements and maintain ground idle noise substantially below current levels. Engine cycle and fan design data were combined to estimate trainer noise levels for Part 36 and idle conditions. A brief description of the noise prediction methods used and the noise levels estimated for the undergraduate trainer are presented in this section.

Estimated noise levels for a PD 418 powered trainer are presented in Table 10 and show that the above noise goals are met.

TABLE 10
Undergraduate trainer noise levels.

FAR Part 36 Levels (EPNdB)

	Takeoff	Approach
Part 36 Requirements	89	98
PD418 Powered Trainer	78	93

Ground Idle Tone Corrected Perceived Noise Levels

PNdBt at 250-ft Radius (Single Engine)

	Front	Rear
T37 with J69-T-25	118.3	99
PD418 Powered Trainer	79	84

Noise estimates were made through a DDA computer program developed for turbofan noise prediction. A noise generation model for each source, fan, jet, turbine, and combustor, is contained in the program so that the noise output from each source is dependent on its individual operating conditions and engine total noise reflects the contribution from each noise source.

High bypass ratio turbofan engines are usually fan noise dominated with the jet and combustor being secondary sources. The PD418 engine incorporates the following design features to reduce fan and jet noise generation:

- o Ample space between the fan and the outlet guide vanes (1.5 fan chords)
- o Ratio of outlet guide vanes to fan blades >2 to cut off blade passing tone
- o Internal mixer to reduce nozzle exit velocity

The noise estimates for the PD418 include the noise reductions provided by these features. The PD418 incorporates a 1.8:1 pressure ratio fan (design point) matched to the GMA500 core and operates at part speed for takeoff, climb, and approach. The engine is fan noise dominated at these conditions so that fan duct acoustic treatment could be used to achieve levels lower than the 78 and 93 EPNdB predicted for takeoff and approach. These levels are 11 and 5 EPNdB below the FAR Part 36 requirements.

At the ground idle condition, the PD418 peak levels at 250-ft radius are expected to be 79 and 84 PNdBt (tone corrected PNdB) in front and rear of the aircraft. In dBA units, front and rear levels are 60 and 67. These levels translate into noise reductions of 34 PNdBt or 35 dBA when the PD418 trainer is compared with the T37B with the J69-T-25 engine.* In predicting the ground idle noise levels, it was assumed that ingested ground level turbulence would prevent cutoff and so the blade passing tone is included in the above levels.

---

*Speakman, J. D., Power R. G., and Lee, R. A., Community Noise Exposure Resulting from Aircraft Operations, AMRL-TR-73-110, Vol. 4, February 1978.

APPENDIX A

AXIAL COMPRESSOR DESIGN SYSTEM

The vector diagram calculation used for axial compressor design assumes an axisymmetric flow field and obtains a solution of the continuity, energy, and radial equilibrium equations. The design analysis is identified as the Axial Compressor Design System (ACDS) Program BD76. Viscous terms are omitted; however, the equations do account for streamline curvature, radial gradients of total enthalpy and entropy, and blade force terms arising from non-radial blade surfaces. Calculations may be performed at the leading or trailing edges of the airfoils by slanting the calculation stations.

Enthalpy rise across a rotor is given by Euler's turbine equation, and the continuity equation is adjusted for local as well as endwall blockage.

Used as a design tool, the calculation provides detailed examination of the aerothermodynamic solution of the flow process through the compressor. The solution is iterative and must rely on profile loss estimates which are correlated as a function of aerodynamic loading (diffusion factor). This data has been obtained from test data for a wide range of compressor designs and is continually updated.

The equilibrium equation is in the form of:

$$\left.\frac{dV_z^2}{dr}\right|_c = -\left.\frac{d(V_\theta^2)}{dr}\right|_c - \left.\frac{d(V_r^2)}{dr}\right|_c + 2\left[\left.\frac{(dH_o)}{dr}\right|_c - T\left.\frac{ds}{dr}\right|_c\right]$$

$$+ 2\left[V_z\left.\frac{dV_r}{dz}\right|_\psi - \frac{V_\theta^2}{r}\right] + 2V_z\left.\frac{dV_z}{dz}\right|_\psi \left.\frac{dz}{dr}\right|_c +$$

$$2V_z\left.\frac{d(rV_\theta)}{dz}\right|_\psi \left.\frac{d\theta}{dr}\right|_c$$

where:

r	radial distance
z	axial distance
θ	tangential distance
V_r	radial velocity
V_z	axial velocity
V_θ	tangential veolicty
T	total temperature
s	entropy
H_θ	total enthalpy
c	projection of the calculating station on relative stress surface
ψ	relative to stream surface

The continuity equation is:

$$W_a = 2\pi \int_{y_h}^{y_t} K_\gamma \, \rho \, V_m \sin(\lambda - \epsilon) \, r dy$$

where:

W_a	airflow
V_m	meridional velocity
K_γ	blockage factor
ρ	density
Y	length along the calculating station
ϵ	angle between tangent to the streamline projected on the meridional plan and axial direction
λ	angle between calculation station and axial

APPENDIX B

DESIGN POINT VECTOR DIAGRAMS

TABLE B-1.

Velocity diagrams.

ROTOR INLET

MASS FLOW RATE	26.37	FLOW RATE/SQ. FT.	42.28 (CORRECTED)	MASS AVE. TOTAL PRESSURE	6.47
CORRECTED FLOW RATE	55.83	ANNULUS AREA	1.32 SQ. FT = 190.2 SQ.IN	MASS AVE. TOTAL TEMPERATURE	451.0

RADIUS INCHES	AXIAL VELOCITY	WHIRL VELOCITY	RADIAL VELOCITY	TOTAL PRESSURE	STATIC PRESSURE	TEMPERATURES TOTAL	TEMPERATURES STATIC	ABSOLUTE VELOCITY	ABSOLUTE MACH NO.	MER. VELOCITY	PERCENT SPAN	S.L. NO.
3.405	516.7	0.0	291.39	6.47	5.11	451.0	421.7	593.2	0.589	593.2	0.2	1
3.815	556.4	0.0	249.52	6.47	5.04	451.0	420.0	609.8	0.607	609.8	8.2	3
4.265	589.3	0.0	209.00	6.47	4.98	451.0	418.4	625.3	0.623	625.3	17.1	5
4.742	615.0	0.0	171.50	6.47	4.92	451.0	417.0	638.5	0.637	638.5	26.5	7
5.239	634.3	0.0	137.46	6.47	4.87	451.0	415.9	649.0	0.649	649.0	36.2	9
5.750	648.1	0.0	106.66	6.47	4.84	451.0	415.0	656.9	0.657	656.9	46.2	11
6.274	657.3	0.0	78.74	6.47	4.82	451.0	414.5	662.0	0.663	662.0	56.5	13
6.808	662.3	0.0	53.38	6.47	4.80	451.0	414.2	664.4	0.666	664.4	67.0	15
7.352	663.7	0.0	30.32	6.47	4.80	451.0	414.2	664.4	0.666	664.4	77.7	17
7.905	662.3	0.0	9.46	6.47	4.81	451.0	414.4	662.3	0.663	662.3	88.6	19
8.467	659.0	0.0	-8.62	6.47	4.83	451.0	414.8	659.0	0.660	659.0	99.6	21

ROTOR EXIT

MASS FLOW RATE	26.37	FLOW RATE/SQ. FT.	30.26 (CORRECTED)	MASS AVE. TOTAL PRESSURE	11.88
CORRECTED FLOW RATE	33.50	ANNULUS AREA	1.11 SQ. FT = 159.4 SQ.IN	MASS AVE. TOTAL TEMPERATURE	548.1
CORRECTED TIP SPEED	1606. FT/SEC			ROTOR ADIABATIC EFFICIENCY	88.4
PRESSURE RATIO	1.837	CUMULATIVE ADIABATIC EFFICIENCY	88.4		

RADIUS INCHES	AXIAL VELOCITY	WHIRL VELOCITY	RADIAL VELOCITY	TOTAL PRESSURE	STATIC PRESSURE	TEMPERATURES TOTAL	TEMPERATURES STATIC	ABSOLUTE VELOCITY	ABSOLUTE MACH NO.	MER. VELOCITY	PERCENT SPAN	S.L. NO.
4.652	598.0	690.4	202.14	12.41	7.51	545.5	472.6	935.5	0.877	631.3	0.3	1
4.855	585.7	650.9	178.66	12.24	7.76	544.0	477.5	893.6	0.834	612.3	5.6	3
5.108	571.3	610.2	154.24	12.10	8.02	542.7	482.5	850.0	0.789	591.7	12.2	5
5.406	555.2	572.5	130.03	11.97	8.27	542.1	487.7	808.1	0.746	570.3	19.9	7
5.744	541.5	536.0	107.49	11.88	8.51	541.6	492.3	769.4	0.707	552.1	28.7	9
6.116	528.9	504.5	86.50	11.82	8.72	541.8	496.7	736.1	0.674	535.9	38.4	11
6.519	517.0	480.7	67.08	11.79	8.91	543.2	501.3	709.1	0.646	521.3	48.8	13
6.949	505.3	464.7	49.30	11.78	9.07	546.1	506.6	688.3	0.624	507.7	60.0	15
7.405	494.3	455.1	33.32	11.80	9.21	550.2	512.5	672.7	0.606	495.4	71.9	17
7.887	481.4	454.7	19.34	11.84	9.34	556.5	520.0	662.5	0.593	481.8	84.4	19
8.399	462.4	466.5	8.40	11.90	9.46	566.3	530.4	656.9	0.582	462.4	97.7	21

RELATIVE INLET	MACH NOS. EXIT	TOTAL TEMP RISE	TOTAL TEMP RATIO	WHEEL SPEED IN	WHEEL SPEED OUT	ROTOR PRESSURE RATIO	ROTOR ADIABATIC EFFICIENCY	ROTOR POLYTROPIC EFFICIENCY	S.L. NO.
0.838	0.605	94.49	1.209	600.9	821.0	1.918	97.8	98.1	1
0.904	0.603	92.97	1.206	673.2	856.7	1.893	97.2	97.5	3
0.975	0.612	91.71	1.203	752.7	901.4	1.870	96.5	96.9	5
1.051	0.636	91.06	1.202	836.9	954.0	1.851	95.4	95.9	7
1.129	0.671	90.58	1.201	924.5	1013.7	1.837	94.6	95.2	9
1.210	0.719	90.80	1.201	1014.7	1079.4	1.827	93.5	94.1	11
1.292	0.773	92.20	1.204	1107.2	1150.4	1.823	91.7	92.5	13
1.375	0.829	95.01	1.211	1201.5	1226.4	1.822	88.9	89.9	15
1.459	0.888	99.15	1.220	1297.5	1306.8	1.824	85.4	86.7	17
1.547	0.943	105.50	1.234	1395.1	1391.9	1.830	80.7	82.4	19
1.635	0.988	115.25	1.256	1494.2	1482.2	1.840	74.6	76.7	21

S.L. NO.	DIFFUSION FACTOR	OMEGA BAR	DELTA PS/Q	SOLIDITY	TOTAL TURNING	ABSOLUTE FLOW ANGLE INLET	ABSOLUTE FLOW ANGLE EXIT	EQUIVALENT DIFFUSION FACTOR	RELATIVE FLOW ANGLE INLET	RELATIVE FLOW ANGLE EXIT	RELATIVE VELOCITY INLET	RELATIVE VELOCITY EXIT	RELATIVE TEMPERATURE INLET	RELATIVE TEMPERATURE EXIT
1	0.477	0.244	0.801	1.960	33.68	0.0	47.56	2.040	45.37	11.69	844.4	644.6	481.	507.
3	0.509	0.048	0.770	1.823	29.25	0.0	46.75	1.958	47.83	18.58	908.4	646.0	489.	512.
5	0.526	0.052	0.727	1.703	24.09	0.0	45.88	1.863	50.28	26.20	978.5	659.5	498.	519.
7	0.530	0.059	0.674	1.595	18.88	0.0	45.11	1.757	52.66	33.78	1052.6	686.1	509.	527.
9	0.519	0.062	0.613	1.504	14.06	0.0	44.15	1.644	54.93	40.87	1129.6	730.1	522.	537.
11	0.500	0.068	0.550	1.428	10.08	0.0	43.27	1.538	57.08	47.01	1208.8	785.9	537.	548.
13	0.481	0.080	0.488	1.371	7.02	0.0	42.68	1.446	59.13	52.10	1290.0	848.7	553.	561.
15	0.462	0.101	0.427	1.329	4.74	0.0	42.47	1.370	61.06	56.31	1372.9	915.4	571.	576.
17	0.444	0.126	0.371	1.302	3.07	0.0	42.57	1.308	62.88	59.82	1457.7	985.3	591.	593.
19	0.432	0.163	0.320	1.287	1.81	0.0	43.34	1.257	64.60	62.79	1544.3	1053.7	613.	612.
21	0.428	0.215	0.276	1.276	0.68	0.0	45.25	1.206	66.20	65.52	1633.1	1116.0	637.	634.

TABLE B-1. (Continued)

STATOR INLET

MASS FLOW RATE	26.37	FLOW RATE/SQ. FT.	31.39 (CORRECTED)	MASS AVE. TOTAL PRESSURE	11.89
CORRECTED FLOW RATE	33.49	ANNULUS AREA	1.07 SQ. FT = 153.7 SQ.IN	MASS AVE. TOTAL TEMPERATURE	547.9

RADIUS INCHES	AXIAL VELOCITY	WHIRL VELOCITY	RADIAL VELOCITY	TOTAL PRESSURE	STATIC PRESSURE	TEMPERATURES TOTAL	TEMPERATURES STATIC	ABSOLUTE VELOCITY	ABSOLUTE MACH NO.	MER. VELOCITY	PERCENT SPAN	S.L. NO.
4.912	625.2	653.8	154.80	12.41	7.67	545.5	475.3	917.8	0.858	644.1	0.3	1
5.108	617.3	618.6	138.16	12.24	7.83	544.0	478.8	884.8	0.825	632.6	5.8	3
5.351	607.3	582.5	119.47	12.10	8.02	542.7	482.6	849.9	0.789	618.9	12.6	5
5.636	595.0	549.1	100.08	11.97	8.21	542.1	486.6	815.8	0.754	603.4	20.5	7
5.957	583.6	516.8	81.69	11.88	8.40	541.6	490.4	783.8	0.722	589.3	29.5	9
6.308	572.0	489.2	64.89	11.82	8.57	541.8	494.3	755.4	0.693	575.7	39.3	11
6.687	559.9	468.6	49.85	11.79	8.74	543.2	498.6	731.8	0.668	562.2	49.8	13
7.092	547.0	455.4	36.42	11.78	8.89	546.1	503.7	712.7	0.648	548.2	61.1	15
7.520	533.5	448.2	24.25	11.80	9.03	550.2	509.7	697.2	0.630	534.1	73.0	17
7.973	517.0	449.8	12.58	11.84	9.18	556.5	517.4	685.4	0.615	517.1	85.7	19
8.455	493.2	463.4	0.14	11.90	9.32	566.3	528.1	676.8	0.601	493.2	99.1	21

STATOR EXIT

MASS FLOW RATE	26.37	FLOW RATE/SQ. FT.	32.97 (CORRECTED)	MASS AVE. TOTAL PRESSURE	11.64
CORRECTED FLOW RATE	34.19	ANNULUS AREA	1.04 SQ. FT = 149.3 SQ.IN	MASS AVE. TOTAL TEMPERATURE	548.0
PRESSURE RATIO	1.800	CUMULATIVE ADIABATIC EFFICIENCY	85.2	STAGE ADIABATIC EFFICIENCY	85.2

RADIUS INCHES	AXIAL VELOCITY	WHIRL VELOCITY	RADIAL VELOCITY	TOTAL PRESSURE	STATIC PRESSURE	TEMPERATURES TOTAL	TEMPERATURES STATIC	ABSOLUTE VELOCITY	ABSOLUTE MACH NO.	MER. VELOCITY	PERCENT SPAN	S.L. NO.
5.170	588.8	0.0	74.07	11.64	9.60	545.5	516.2	593.5	0.533	593.5	0.6	1
5.341	578.6	0.0	64.44	11.64	9.66	544.0	515.8	582.1	0.523	582.1	5.7	3
5.558	567.1	0.0	54.47	11.64	9.74	542.7	515.7	569.7	0.512	569.7	12.2	5
5.816	555.5	0.0	44.98	11.64	9.81	542.1	516.2	557.3	0.500	557.3	19.9	7
6.111	544.4	0.0	36.44	11.64	9.88	541.6	516.8	545.6	0.489	545.6	28.8	9
6.440	534.5	0.0	29.08	11.64	9.95	541.8	518.0	535.3	0.480	535.3	38.6	11
6.799	526.5	0.0	22.67	11.65	10.00	543.2	520.1	527.0	0.471	527.0	49.4	13
7.183	520.8	0.0	16.84	11.64	10.04	546.1	523.4	521.1	0.465	521.1	60.9	15
7.589	517.7	0.0	11.19	11.64	10.07	550.2	527.9	517.8	0.460	517.8	73.1	17
8.014	517.6	0.0	5.43	11.64	10.09	556.5	534.2	517.7	0.457	517.7	85.8	19
8.456	522.0	0.0	-0.73	11.64	10.09	566.3	543.6	522.0	0.457	522.0	99.1	21

ABSOLUTE MACH NOS. INLET	ABSOLUTE MACH NOS. EXIT	TOTAL TEMP RISE	TOTAL TEMP RATIO	WHEEL SPEED IN	WHEEL SPEED OUT	STAGE PRESSURE RATIO	STAGE ADIABATIC EFFICIENCY	STAGE POLYTROPIC EFFICIENCY	
0.858	0.533	94.49	1.209	0.0	0.0	1.800	87.4	88.5	1
0.925	0.523	92.97	1.206	0.0	0.0	1.800	88.9	89.8	3
0.789	0.512	91.71	1.203	0.0	0.0	1.800	90.1	90.9	5
0.754	0.500	91.06	1.202	0.0	0.0	1.800	90.7	91.5	7
0.722	0.489	90.58	1.201	0.0	0.0	1.800	91.2	91.9	9
0.693	0.480	90.80	1.201	0.0	0.0	1.800	91.0	91.7	11
0.668	0.471	92.20	1.204	0.0	0.0	1.800	89.6	90.5	13
0.648	0.465	95.01	1.211	0.0	0.0	1.800	87.0	88.0	15
0.630	0.460	99.15	1.220	0.0	0.0	1.800	83.3	84.6	17
0.615	0.457	105.50	1.234	0.0	0.0	1.800	78.3	80.0	19
0.601	0.457	115.25	1.256	0.0	0.0	1.800	71.7	73.9	21

S.L. NO.	DIFFUSION FACTOR	OMEGA BAR	DELTA PS/Q	SOLIDITY	TOTAL TURNING	ABSOLUTE FLOW ANGLE INLET	ABSOLUTE FLOW ANGLE EXIT	EQUIVALENT DIFFUSION FACTOR
1	0.549	0.161	0.407	1.776	45.43	45.43	0.0	1.869
3	0.539	0.136	0.415	1.735	44.36	44.36	0.0	1.834
5	0.529	0.111	0.421	1.687	43.26	43.26	0.0	1.802
7	0.519	0.088	0.426	1.636	42.31	42.31	0.0	1.777
9	0.510	0.068	0.427	1.583	41.25	41.25	0.0	1.752
11	0.501	0.054	0.423	1.531	40.36	40.36	0.0	1.735
13	0.494	0.047	0.414	1.480	39.81	39.81	0.0	1.725
15	0.490	0.048	0.399	1.432	39.71	39.71	0.0	1.730
17	0.488	0.057	0.375	1.386	40.00	40.00	0.0	1.746
19	0.488	0.074	0.343	1.343	41.02	41.02	0.0	1.783
21	0.491	0.099	0.298	1.303	43.21	43.21	0.0	1.857

APPENDIX C

ROTOR AND STATOR BLADE COORDINATES

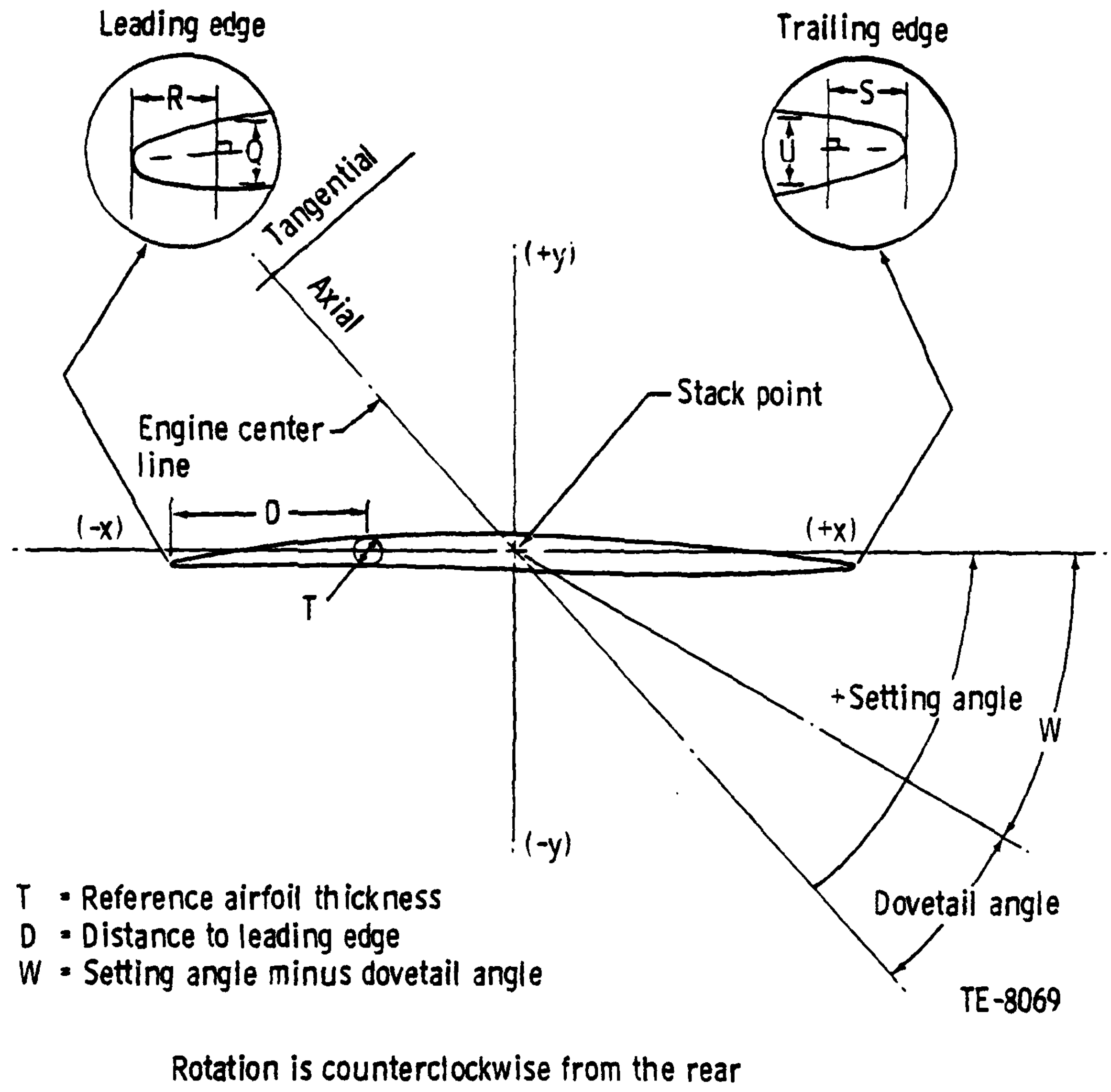

Figure C-1. Blade manufacturing dimension definitions.

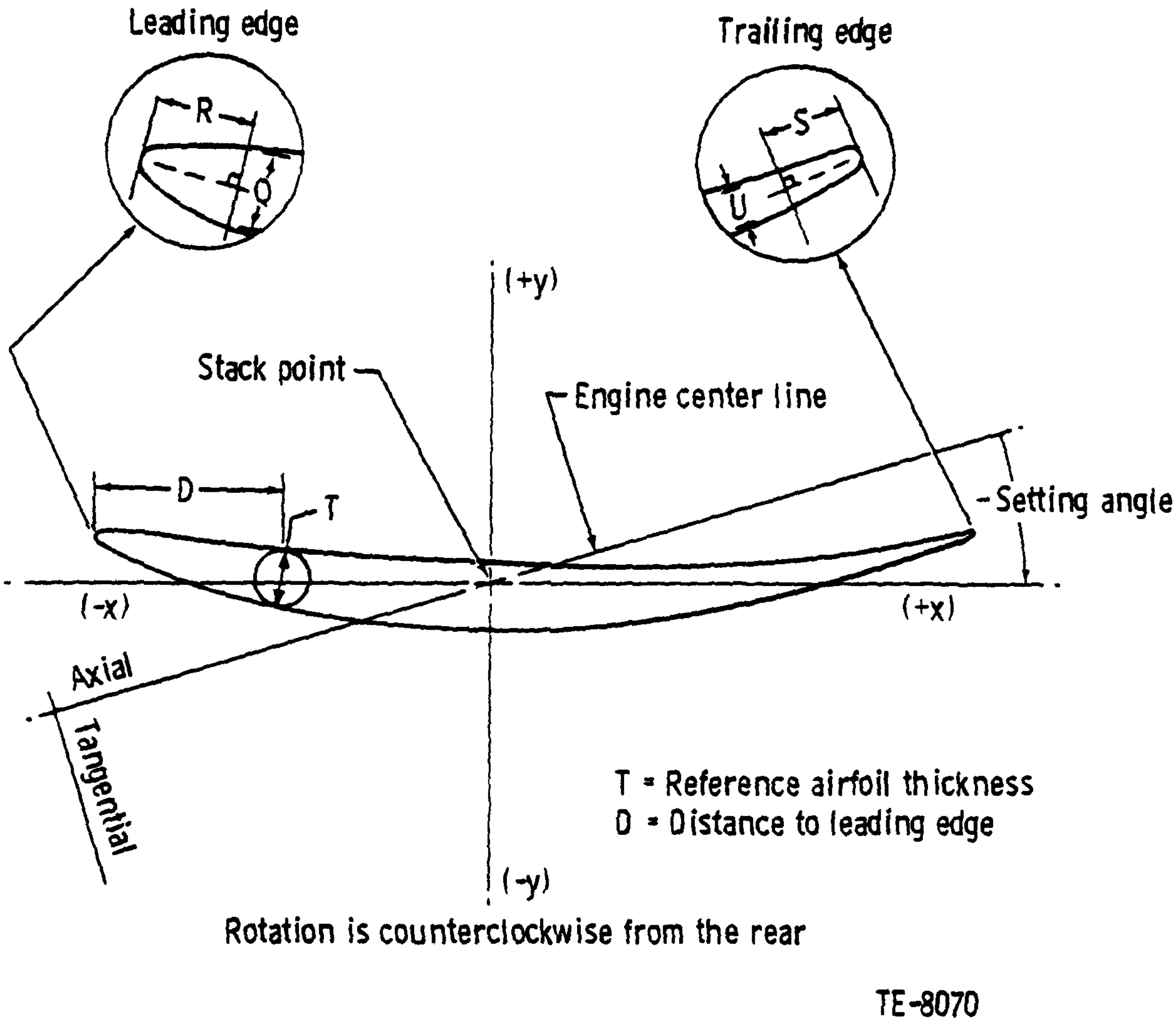

Figure C-2. Vane manufacturing dimension definitions.

23 AUG 79 PAGE 1

FAN COMPRESSOR BLACE CBC 12120

RADIAL DISTANCE	SETTING ANGLE	REFERENCE AIRFOIL THICKNESS	DISTANCE TO LEADING EDGE	RADII L.E.	RADII T.E.
3.2500	-9.175 -9C 10M 28S	0.2982	1.3000	0.014	0.015

LEADING EDGE AXIAL TANGENT POINT -0.9448

Q DIMENSICN 0.0368 U DIMENSION 0.0322
R DIMENSICN 0.0600 S DIMENSION 0.0600

STACK PCINT CCORDINATES 0.0 , 0.0
CENTER CF GRAVITY CCORDINATES 0.1476, -0.0879
CCMPRESSOR ROTATION IS COUNTER CLOCKWISE FROM THE REAR

REFERENCE COORCINATE POINTS

STATICN NO.	X	Y		X	Y		X	Y
1	-0.8491*	-0.6670	21	0.4213	0.1936	41	0.4470	-0.1149
2	-0.8472	-0.6594	22	0.5064	0.1567	42	0.3554	-0.0916
3	-0.8133	-0.5831	23	0.5919	0.1073	43	0.2831	-0.0802
4	-0.7769	-0.5081	24	0.6987	0.0266	44	0.1943	-0.0743
5	-0.7276	-0.4167	25	0.7836	-0.0540	45	0.1243	-0.0759
6	-0.6850	-0.3457	26	0.8675	-0.1494	46	0.0556	-0.0828
7	-0.6396	-0.2769	27	0.9703	-0.2901	47	-0.0286	-0.0982
8	-0.5789	-0.1943	28	1.0501	-0.4210	48	-0.0940	-0.1160
9	-0.5271	-0.1314	29	1.1461	-0.6077	49	-0.1579	-0.1386
10	-0.4724	-0.0717	30	1.1643	-0.6482	50	-0.2360	-0.1729
11	-0.3998	-0.0023	31	1.1706*	-0.6664	51	-0.2969	-0.2048
12	-0.3383	0.0486	32	1.1469	-0.6659	52	-0.3713	-0.2499
13	-0.2574	0.1056	33	1.1267	-0.6388	53	-0.4294	-0.2898
14	-0.1893	0.1453	34	1.0250	-0.5158	54	-0.4864	-0.3329
15	-0.1181	0.1789	35	0.9448	-0.4311	55	-0.5560	-0.3907
16	-0.0250	0.2112	36	0.8461	-0.3410	56	-0.6105	-0.4400
17	0.0521	0.2282	37	0.7682	-0.2799	57	-0.6639	-0.4918
18	0.1314	0.2372	38	0.6913	-0.2277	58	-0.7292	-0.5598
19	0.2329	0.2359	39	0.5962	-0.1745	59	-0.7803	-0.6166
20	0.3160	0.2237	40	0.5212	-0.1410	60	-0.8304	-0.6754

* INDICATES EXTREME POINTS

23 AUG 79 PAGE 3

FAN COMPRESSOR BLACE CBC 12120

RADIAL DISTANCE	SETTING ANGLE	REFERENCE AIRFOIL THICKNESS	DISTANCE TO LEADING EDGE	RADII L.E.	RADII T.E.
3.9500	11.933 11D 55M 58S	0.2241	1.3000	0.013	0.014

LEADING EDGE AXIAL TANGENT POINT -0.9108

Q DIMENSICN 0.0337 U DIMENSION 0.0321
R DIMENSICN 0.0600 S DIMENSION 0.0600

STACK PCINT CCORDINATES 0.0 , 0.0
CENTER CF GRAVITY COORDINATES 0.0754, -0.0674
COMPRESSOR ROTATION IS COUNTER CLOCKWISE FROM THE REAR

REFERENCE COORCINATE POINTS

STATION NO.	X	Y		X	Y		X	Y
1	-1.0362*	-0.5001	21	0.4402	0.1430	41	0.4084	-0.0731
2	-1.0310	-0.4886	22	0.5133	0.1149	42	0.3245	-0.0556
3	-0.9711	-0.4315	23	0.5840	0.0776	43	0.2567	-0.0475
4	-0.9101	-0.3758	24	0.6683	0.0172	44	0.1712	-0.0442
5	-0.8322	-0.3083	25	0.7317	-0.0429	45	0.1025	-0.0468
6	-0.7685	-0.2561	26	0.7910	-0.1137	46	0.0336	-0.0539
7	-0.7035	-0.2056	27	0.8585	-0.2180	47	-0.0531	-0.0687
8	-0.6199	-0.1441	28	0.9064	-0.3148	48	-0.1228	-0.0846
9	-0.5514	-0.0973	29	0.9577	-0.4526	49	-0.1925	-0.1038
10	-0.4818	-0.0531	30	0.9665	-0.4823	50	-0.2797	-0.1320
11	-0.3929	-0.0018	31	0.9691*	-0.4940	51	-0.3494	-0.1577
12	-0.3205	0.0358	32	0.9520	-0.4959	52	-0.4364	-0.1933
13	-0.2284	0.0780	33	0.9393	-0.4791	53	-0.5059	-0.2244
14	-0.1536	0.1073	34	0.8721	-0.3839	54	-0.5752	-0.2576
15	-0.0780	0.1324	35	0.8157	-0.3182	55	-0.6617	-0.3018
16	0.0178	0.1569	36	0.7423	-0.2481	56	-0.7306	-0.3391
17	0.0954	0.1702	37	0.6816	-0.2066	57	-0.7987	-0.3773
18	0.1731	0.1769	38	0.6194	-0.1601	58	-0.8837	-0.4267
19	0.2698	0.1756	39	0.5397	-0.1190	59	-0.9515	-0.4675
20	0.3463	0.1661	40	0.4746	-0.0931	60	-1.0192	-0.5093

* INDICATES EXTREME POINTS

23 AUG 79 PAGE 5

FAN COMPRESSOR BLADE CBC 12120

RADIAL DISTANCE	SETTING ANGLE	REFERENCE AIRFOIL THICKNESS	DISTANCE TO LEADING EDGE	RADII L.E.	RADII T.E.
4.6500	29.957 29D 57M 25S	0.1476	1.3000	0.013	0.014

LEADING EDGE AXIAL TANGENT POINT -0.8742

Q DIMENSION 0.0323 U DIMENSION 0.0375
R DIMENSION 0.0600 S DIMENSION 0.0600

STACK POINT COORDINATES 0.0 , 0.0
CENTER OF GRAVITY COORDINATES 0.0286, -0.0344
COMPRESSOR ROTATION IS COUNTER CLOCKWISE FROM THE REAR

REFERENCE COORDINATE POINTS

STATION NO.	X	Y		X	Y		X	Y
1	-1.1771*	-0.2956	21	0.4744	0.1136	41	0.4503	-0.0263
2	-1.1685	-0.2827	22	0.5525	0.0970	42	0.3575	-0.0183
3	-1.0928	-0.2472	23	0.6287	0.0747	43	0.2824	-0.0161
4	-1.0167	-0.2127	24	0.7205	0.0382	44	0.1877	-0.0181
5	-0.9210	-0.1713	25	0.7906	0.0017	45	0.1115	-0.0236
6	-0.8441	-0.1395	26	0.8554	-0.0425	46	0.0351	-0.0323
7	-0.7667	-0.1089	27	0.9283	-0.1086	47	-0.0619	-0.0473
8	-0.6695	-0.0726	28	0.9802	-0.1703	48	-0.1403	-0.0610
9	-0.5913	-0.0452	29	1.0359	-0.2586	49	-0.2186	-0.0757
10	-0.5127	-0.0191	30	1.0457	-0.2778	50	-0.3166	-0.0952
11	-0.4140	0.0112	31	1.0482*	-0.2879	51	-0.3950	-0.1118
12	-0.3347	0.0337	32	1.0318	-0.2996	52	-0.4931	-0.1335
13	-0.2352	0.0594	33	1.0191	-0.2858	53	-0.5716	-0.1517
14	-0.1552	0.0780	34	0.9514	-0.2228	54	-0.6501	-0.1705
15	-0.0751	0.0947	35	0.8936	-0.1753	55	-0.7484	-0.1949
16	0.0260	0.1129	36	0.8171	-0.1328	56	-0.8270	-0.2151
17	0.1085	0.1236	37	0.7529	-0.1015	57	-0.9057	-0.2358
18	0.1910	0.1299	38	0.6843	-0.0764	58	-1.0042	-0.2623
19	0.2934	0.1311	39	0.5959	-0.0518	59	-1.0831	-0.2841
20	0.3746	0.1266	40	0.5236	-0.0370	60	-1.1621	-0.3062

* INDICATES EXTREME POINTS

23 AUG 79 PAGE 7

FAN COMPRESSOR BLADE CBC 12120

RADIAL DISTANCE	SETTING ANGLE	REFERENCE AIRFOIL THICKNESS	DISTANCE TO LEADING EDGE	RADII L.E.	RADII T.E.
5.4000	43.936 43D 56M 9S	0.1180	1.3000	0.013	0.013

LEADING EDGE AXIAL TANGENT POINT -0.8401

Q DIMENSION 0.0305 U DIMENSION 0.0356
R DIMENSION 0.0600 S DIMENSION 0.0600

STACK POINT COORDINATES 0.0 , 0.0
CENTER OF GRAVITY COORDINATES 0.0196, -0.0104
COMPRESSOR ROTATION IS COUNTER CLOCKWISE FROM THE REAR

REFERENCE COORDINATE POINTS

STATION NO.	X	Y		X	Y		X	Y
1	-1.2862*	-0.1293	21	0.4983	0.0782	41	0.4873	-0.0303
2	-1.2752	-0.1162	22	0.5832	0.0691	42	0.3832	-0.0273
3	-1.1900	-0.0965	23	0.6675	0.0574	43	0.2998	-0.0266
4	-1.1049	-0.0776	24	0.7720	0.0386	44	0.1953	-0.0278
5	-0.9984	-0.0552	25	0.8547	0.0203	45	0.1116	-0.0302
6	-0.9132	-0.0383	26	0.9364	-0.0012	46	0.0278	-0.0341
7	-0.8279	-0.0223	27	1.0369	-0.0327	47	-0.0779	-0.0401
8	-0.7213	-0.0036	28	1.1158	-0.0620	48	-0.1627	-0.0453
9	-0.6360	0.0102	29	1.2121	-0.1041	49	-0.2475	-0.0508
10	-0.5507	0.0231	30	1.2310	-0.1133	50	-0.3536	-0.0582
11	-0.4440	0.0378	31	1.2388*	-0.1253	51	-0.4386	-0.0645
12	-0.3587	0.0485	32	1.2223	-0.1352	52	-0.5449	-0.0726
13	-0.2518	0.0605	33	1.2024	-0.1335	53	-0.6301	-0.0795
14	-0.1663	0.0690	34	1.1024	-0.1081	54	-0.7154	-0.0866
15	-0.0808	0.0763	35	1.0217	-0.0908	55	-0.8221	-0.0959
16	0.0262	0.0839	36	0.9201	-0.0725	56	-0.9077	-0.1038
17	0.1123	0.0882	37	0.8384	-0.0604	57	-0.9933	-0.1120
18	0.1984	0.0902	38	0.7562	-0.0503	58	-1.1005	-0.1227
19	0.3059	0.0893	39	0.6531	-0.0464	59	-1.1865	-0.1316
20	0.3916	0.0860	40	0.5703	-0.0345	60	-1.2725	-0.1408

* INDICATES EXTREME POINTS

FAN COMPRESSOR BLADE CBC 12120

RADIAL DISTANCE	SETTING ANGLE	REFERENCE AIRFOIL THICKNESS	DISTANCE TO LEADING EDGE	RADII L.E.	RADII T.E.
6.4000	54.367 54D 22M 2S	0.0933	1.3000	0.013	0.013

LEADING EDGE AXIAL TANGENT POINT -0.8147

Q DIMENSION 0.0287 U DIMENSION 0.0318
R DIMENSION 0.0600 S DIMENSION 0.0600

STACK POINT COORDINATES 0.0 , 0.0
CENTER OF GRAVITY COORDINATES 0.0127, 0.0167
COMPRESSOR ROTATION IS COUNTER CLOCKWISE FROM THE REAR

REFERENCE COORDINATE POINTS

STATION NO.	X	Y	STATION NO.	X	Y	STATION NO.	X	Y
1	-1.4171*	-0.0197	21	0.5151	0.0744	41	0.5118	-0.0167
2	-1.4048	-0.0071	22	0.6071	0.0706	42	0.3978	-0.0170
3	-1.3109	0.0016	23	0.6990	0.0654	43	0.3066	-0.0177
4	-1.2172	0.0098	24	0.8138	0.0571	44	0.1924	-0.0192
5	-1.1004	0.0194	25	0.9054	0.0490	45	0.1007	-0.0202
6	-1.0071	0.0265	26	0.9969	0.0397	46	0.0090	-0.0212
7	-0.9140	0.0332	27	1.1112	0.0264	47	-0.1057	-0.0222
8	-0.7979	0.0408	28	1.2024	0.0143	48	-0.1976	-0.0230
9	-0.7052	0.0463	29	1.3162	-0.0025	49	-0.2896	-0.0236
10	-0.6126	0.0514	30	1.3389	-0.0061	50	-0.4047	-0.0244
11	-0.4971	0.0571	31	1.3499*	-0.0187	51	-0.4969	-0.0250
12	-0.4048	0.0611	32	1.3357	-0.0318	52	-0.6123	-0.0257
13	-0.2896	0.0655	33	1.3126	-0.0311	53	-0.7049	-0.0262
14	-0.1975	0.0686	34	1.1977	-0.0277	54	-0.7975	-0.0268
15	-0.1055	0.0713	35	1.1060	-0.0252	55	-0.9136	-0.0276
16	0.0093	0.0740	36	0.9914	-0.0225	56	-1.0067	-0.0283
17	0.1012	0.0758	37	0.8999	-0.0207	57	-1.0999	-0.0290
18	0.1929	0.0772	38	0.8085	-0.0191	58	-1.2168	-0.0300
19	0.3079	0.0781	39	0.6943	-0.0177	59	-1.3105	-0.0309
20	0.4000	0.0773	40	0.6031	-0.0170	60	-1.4045	-0.0319

* INDICATES EXTREME POINTS

FAN COMPRESSOR BLADE CBC 12120

RADIAL DISTANCE	SETTING ANGLE	REFERENCE AIRFOIL THICKNESS	DISTANCE TO LEADING EDGE	RADII L.E.	RADII T.E.
7.4000	60.445 60D 26M 43S	0.0787	1.3000	0.011	0.011

LEADING EDGE AXIAL TANGENT POINT -0.8169

Q DIMENSION 0.0258 U DIMENSION 0.0286
R DIMENSION 0.0600 S DIMENSION 0.0600

STACK POINT COORDINATES 0.0 , 0.0
CENTER OF GRAVITY COORDINATES 0.0183, 0.0467
COMPRESSOR ROTATION IS COUNTER CLOCKWISE FROM THE REAR

REFERENCE COORDINATE POINTS

STATION NO.	X	Y	STATION NO.	X	Y	STATION NO.	X	Y
1	-1.5796*	0.0365	21	0.5475	0.0941	41	0.5464	0.0100
2	-1.5677	0.0484	22	0.6490	0.0932	42	0.4203	0.0080
3	-1.4635	0.0529	23	0.7506	0.0912	43	0.3192	0.0068
4	-1.3596	0.0571	24	0.8777	0.0873	44	0.1929	0.0058
5	-1.2303	0.0619	25	0.9795	0.0829	45	0.0919	0.0054
6	-1.1273	0.0654	26	1.0814	0.0776	46	-0.0092	0.0054
7	-1.0245	0.0686	27	1.2090	0.0695	47	-0.1355	0.0056
8	-0.8964	0.0723	28	1.3112	0.0620	48	-0.2367	0.0061
9	-0.7942	0.0750	29	1.4393	0.0512	49	-0.3380	0.0068
10	-0.6923	0.0774	30	1.4649	0.0488	50	-0.4647	0.0080
11	-0.5652	0.0801	31	1.4755*	0.0382	51	-0.5662	0.0091
12	-0.4636	0.0820	32	1.4631	0.0258	52	-0.6934	0.0107
13	-0.3369	0.0842	33	1.4373	0.0252	53	-0.7954	0.0122
14	-0.2357	0.0857	34	1.3086	0.0225	54	-0.8975	0.0138
15	-0.1346	0.0872	35	1.2061	0.0205	55	-1.0256	0.0158
16	-0.0083	0.0888	36	1.0784	0.0183	56	-1.1283	0.0176
17	0.0926	0.0900	37	0.9766	0.0166	57	-1.2313	0.0194
18	0.1936	0.0912	38	0.8751	0.0150	58	-1.3605	0.0218
19	0.3198	0.0926	39	0.7485	0.0131	59	-1.4642	0.0237
20	0.4208	0.0936	40	0.6474	0.0116	60	-1.5683	0.0257

* INDICATES EXTREME POINTS

FAN COMPRESSOR BLADE CBC 12120

RADIAL DISTANCE	SETTING ANGLE	REFERENCE AIRFOIL THICKNESS	DISTANCE TO LEADING EDGE	RADII L.E.	RADII T.E.
8.2500	64.569 64D 34M 7S	0.0724	1.3000	0.010	0.010

LEADING EDGE AXIAL TANGENT POINT -0.8253

Q DIMENSION 0.0231 U DIMENSION 0.0264
R DIMENSION 0.0600 S DIMENSION 0.0600

STACK POINT COORDINATES 0.0 , 0.0
CENTER OF GRAVITY COORDINATES 0.0310, 0.0733
COMPRESSOR ROTATION IS COUNTER CLOCKWISE FROM THE REAR

REFERENCE COORDINATE POINTS

STATION NO.	X	Y	STATION NO.	X	Y	STATION NO.	X	Y
1	-1.7497*	0.0754	21	0.5793	0.1184	41	0.5790	0.0340
2	-1.7387	0.0859	22	0.6908	0.1198	42	0.4401	0.0313
3	-1.6245	0.0883	23	0.8025	0.1199	43	0.3290	0.0298
4	-1.5107	0.0905	24	0.9424	0.1183	44	0.1903	0.0287
5	-1.3690	0.0931	25	1.0545	0.1156	45	0.0794	0.0283
6	-1.2561	0.0949	26	1.1669	0.1117	46	-0.0315	0.0284
7	-1.1435	0.0966	27	1.3076	0.1051	47	-0.1702	0.0290
8	-1.0032	0.0985	28	1.4205	0.0984	48	-0.2811	0.0300
9	-0.8913	0.0998	29	1.5619	0.0884	49	-0.3921	0.0313
10	-0.7797	0.1011	30	1.5903	0.0861	50	-0.5311	0.0334
11	-0.6404	0.1026	31	1.5998*	0.0762	51	-0.6424	0.0353
12	-0.5292	0.1037	32	1.5889	0.0658	52	-0.7817	0.0382
13	-0.3904	0.1051	33	1.5604	0.0646	53	-0.8934	0.0407
14	-0.2795	0.1062	34	1.4183	0.0586	54	-1.0053	0.0435
15	-0.1686	0.1073	35	1.3051	0.0544	55	-1.1455	0.0472
16	-0.0302	0.1089	36	1.1644	0.0496	56	-1.2580	0.0504
17	0.0805	0.1102	37	1.0522	0.0461	57	-1.3708	0.0537
18	0.1912	0.1117	38	0.9404	0.0429	58	-1.5122	0.0581
19	0.3297	0.1138	39	0.8011	0.0392	59	-1.6258	0.0617
20	0.4406	0.1158	40	0.6899	0.0365	60	-1.7398	0.0655

* INDICATES EXTREME POINTS

FAN COMPRESSOR BLADE CBC 12120

RADIAL DISTANCE	SETTING ANGLE	REFERENCE AIRFOIL THICKNESS	DISTANCE TO LEADING EDGE	RADII L.E.	RADII T.E.
8.7500	66.695 66D 41M 41S	0.0698	1.3000	0.010	0.009

LEADING EDGE AXIAL TANGENT POINT -0.8293

Q DIMENSION 0.0216 U DIMENSION 0.0253
R DIMENSION 0.0600 S DIMENSION 0.0600

STACK POINT COORDINATES 0.0 , 0.0
CENTER OF GRAVITY COORDINATES 0.0421, 0.0897
COMPRESSOR ROTATION IS COUNTER CLOCKWISE FROM THE REAR

REFERENCE COORDINATE POINTS

STATION NO.	X	Y	STATION NO.	X	Y	STATION NO.	X	Y
1	-1.8537*	0.0981	21	0.5981	0.1345	41	0.5983	0.0486
2	-1.8435	0.1079	22	0.7158	0.1373	42	0.4515	0.0456
3	-1.7232	0.1091	23	0.8338	0.1386	43	0.3344	0.0439
4	-1.6035	0.1103	24	0.9816	0.1382	44	0.1881	0.0426
5	-1.4544	0.1116	25	1.1001	0.1363	45	0.0711	0.0421
6	-1.3355	0.1126	26	1.2188	0.1330	46	-0.0458	0.0422
7	-1.2170	0.1134	27	1.3676	0.1268	47	-0.1919	0.0430
8	-1.0693	0.1144	28	1.4870	0.1203	48	-0.3089	0.0442
9	-0.9515	0.1152	29	1.6367	0.1101	49	-0.4258	0.0458
10	-0.8339	0.1159	30	1.6667	0.1078	50	-0.5722	0.0483
11	-0.6873	0.1169	31	1.6757*	0.0988	51	-0.6894	0.0508
12	-0.5701	0.1177	32	1.6658	0.0891	52	-0.8362	0.0543
13	-0.4239	0.1187	33	1.6355	0.0874	53	-0.9538	0.0574
14	-0.3071	0.1197	34	1.4850	0.0798	54	-1.0716	0.0609
15	-0.1904	0.1208	35	1.3653	0.0743	55	-1.2192	0.0655
16	-0.0445	0.1224	36	1.2165	0.0681	56	-1.3376	0.0695
17	0.0722	0.1239	37	1.0980	0.0637	57	-1.4563	0.0737
18	0.1890	0.1257	38	0.9799	0.0596	58	-1.6051	0.0793
19	0.3349	0.1282	39	0.8328	0.0550	59	-1.7247	0.0840
20	0.4518	0.1337	40	0.7154	0.0517	60	-1.8446	0.0889

* INDICATES EXTREME POINTS

FAN COMPRESSOR VANE CSC 12122

RADIAL DISTANCE	SETTING ANGLE	REFERENCE AIRFOIL THICKNESS	DISTANCE TO LEADING EDGE	RADII L.E.	RADII T.E.
4.5009	-24.991 -240 59M 26S	0.0696	0.7450	0.008	0.006

LEADING EDGE AXIAL TANGENT POINT -0.6227

Q DIMENSION 0.0242 U DIMENSION 0.0215
R DIMENSION 0.0600 S DIMENSION 0.0600

STACK POINT COORDINATES 0.0 , 0.0
CENTER OF GRAVITY COORDINATES -0.1199, -0.0516
COMPRESSOR ROTATION IS COUNTER CLOCKWISE FROM THE REAR

REFERENCE COORDINATE POINTS

STATION NO.	X	Y		X	Y		X	Y
1	-0.7152*	0.0645	21	0.1320	-0.0459	41	0.1474	-0.1068
2	-0.7059	0.0692	22	0.1704	-0.0396	42	0.0963	-0.1167
3	-0.6650	0.0573	23	0.2085	-0.0318	43	0.0547	-0.1222
4	-0.6241	0.0459	24	0.2553	-0.0199	44	0.0020	-0.1260
5	-0.5730	0.0325	25	0.2923	-0.0096	45	-0.0406	-0.1265
6	-0.5322	0.0223	26	0.3266	0.0043	46	-0.0835	-0.1247
7	-0.4913	0.0127	27	0.3731	0.0225	47	-0.1366	-0.1197
8	-0.4402	0.0015	28	0.4079	0.0389	48	-0.1787	-0.1143
9	-0.3994	-0.0068	29	0.4503	0.0616	49	-0.2208	-0.1079
10	-0.3585	-0.0146	30	0.4586	0.0664	50	-0.2734	-0.0982
11	-0.3076	-0.0235	31	0.4661*	0.0616	51	-0.3153	-0.0892
12	-0.2668	-0.0300	32	0.4644	0.0580	52	-0.3675	-0.0765
13	-0.2159	-0.0374	33	0.4572	0.0514	53	-0.4091	-0.0650
14	-0.1752	-0.0427	34	0.4194	0.0201	54	-0.4504	-0.0524
15	-0.1345	-0.0474	35	0.3874	-0.0030	55	-0.5016	-0.0352
16	-0.0942	-0.0523	36	0.3453	-0.0294	56	-0.5422	-0.0203
17	-0.0445	-0.0546	37	0.3101	-0.0484	57	-0.5825	-0.0042
18	-0.0049	-0.0554	38	0.2736	-0.0654	58	-0.6323	0.0173
19	0.0443	-0.0542	39	0.2263	-0.0839	59	-0.6717	0.0357
20	0.0835	-0.0515	40	0.1873	-0.0964	60	-0.7105	0.0551

* INDICATES EXTREME POINTS

FAN COMPRESSOR VANE CSC 12122

RADIAL DISTANCE	SETTING ANGLE	REFERENCE AIRFOIL THICKNESS	DISTANCE TO LEADING EDGE	RADII L.E.	RADII T.E.
4.8500	-23.613 -230 37M 3S	0.0753	0.7450	0.008	0.005

LEADING EDGE AXIAL TANGENT POINT -0.5719

Q DIMENSION 0.0248 U DIMENSION 0.0221
R DIMENSION 0.0600 S DIMENSION 0.0600

STACK POINT COORDINATES 0.0 , 0.0
CENTER OF GRAVITY COORDINATES -0.0469, -0.0171
COMPRESSOR ROTATION IS COUNTER CLOCKWISE FROM THE REAR

REFERENCE COORDINATE POINTS

STATION NO.	X	Y		X	Y		X	Y
1	-0.6658*	0.0969	21	0.2119	-0.0092	41	0.2268	-0.0744
2	-0.6564	0.1038	22	0.2520	-0.0032	42	0.1735	-0.0844
3	-0.6141	0.0923	23	0.2919	0.0044	43	0.1302	-0.0899
4	-0.5717	0.0813	24	0.3410	0.0161	44	0.0753	-0.0936
5	-0.5188	0.0683	25	0.3799	0.0272	45	0.0311	-0.0940
6	-0.4765	0.0585	26	0.4183	0.0398	46	-0.0134	-0.0922
7	-0.4342	0.0492	27	0.4654	0.0578	47	-0.0683	-0.0870
8	-0.3814	0.0383	28	0.5025	0.0739	48	-0.1119	-0.0816
9	-0.3392	0.0302	29	0.5473	0.0963	49	-0.1555	-0.0750
10	-0.2969	0.0226	30	0.5567	0.1010	50	-0.2098	-0.0652
11	-0.2442	0.0138	31	0.5644*	0.0963	51	-0.2531	-0.0561
12	-0.2020	0.0074	32	0.5625	0.0923	52	-0.3070	-0.0432
13	-0.1493	0.0001	33	0.5547	0.0856	53	-0.3499	-0.0316
14	-0.1071	-0.0052	34	0.5141	0.0538	54	-0.3925	-0.0189
15	-0.0650	-0.0099	35	0.4799	0.0304	55	-0.4454	-0.0015
16	-0.0129	-0.0149	36	0.4352	0.0037	56	-0.4873	0.0136
17	0.0283	-0.0173	37	0.3979	-0.0155	57	-0.5289	0.0298
18	0.0693	-0.0182	38	0.3593	-0.0327	58	-0.5803	0.0515
19	0.1205	-0.0172	39	0.3096	-0.0514	59	-0.6209	0.0701
20	0.1613	-0.0146	40	0.2686	-0.0640	60	-0.6611	0.0897

* INDICATES EXTREME POINTS

FAN COMPRESSOR VANE CSC 12122

RADIAL DISTANCE	SETTING ANGLE	REFERENCE AIRFOIL THICKNESS	DISTANCE TO LEADING EDGE	RADII L.E.	RADII T.E.
5.1500	-22.567 -22D 33M 54S	0.0800	0.7450	0.008	0.005

LEADING EDGE AXIAL TANGENT POINT -0.5277

Q DIMENSION 0.0252 U DIMENSION 0.0225
R DIMENSION 0.0600 S DIMENSION 0.0600

STACK POINT COORDINATES 0.0 , 0.0
CENTER OF GRAVITY COORDINATES 0.3169, 0.0099
COMPRESSOR ROTATION IS COUNTER CLOCKWISE FROM THE REAR

REFERENCE COORDINATE POINTS

STATION NO.	X	Y		X	Y		X	Y
1	-0.6223*	0.1242	21	0.2817	0.0198	41	0.2963	-0.0491
2	-0.6128	0.1311	22	0.3233	0.0257	42	0.2410	-0.0592
3	-0.5693	0.1193	23	0.3647	0.0331	43	0.1962	-0.0647
4	-0.5257	0.1090	24	0.4159	0.0446	44	0.1395	-0.0684
5	-0.4713	0.0963	25	0.4564	0.0555	45	0.0939	-0.0688
6	-0.4278	0.0866	26	0.4965	0.0679	46	0.0480	-0.0669
7	-0.3843	0.0775	27	0.5459	0.0857	47	-0.0086	-0.0617
8	-0.3300	0.0666	28	0.5848	0.1016	48	-0.0534	-0.0562
9	-0.2865	0.0589	29	0.6326	0.1237	49	-0.0983	-0.0496
10	-0.2430	0.0515	30	0.6421	0.1284	50	-0.1541	-0.0397
11	-0.1397	0.0429	31	0.6499*	0.1235	51	-0.1996	-0.0306
12	-0.1452	0.0366	32	0.6478	0.1193	52	-0.2540	-0.0175
13	-0.0910	0.0294	33	0.6395	0.1126	53	-0.2981	-0.0059
14	-0.0476	0.0242	34	0.5966	0.0904	54	-0.3419	0.0069
15	-0.0042	0.0195	35	0.5605	0.0567	55	-0.3962	0.0245
16	0.0495	0.0145	36	0.5135	0.0297	56	-0.4392	0.0399
17	0.0920	0.0121	37	0.4744	0.0133	57	-0.4819	0.0563
18	0.1343	[illegible]	38	[illegible]	-0.0071	58	-0.5346	0.0783
19	0.1372	0.0122	39	0.3823	-0.0259	59	-0.5763	0.0971
20	0.2293	0.0145	40	0.3397	-0.0386	60	-0.6175	0.1169

* INDICATES EXTREME POINTS

FAN COMPRESSOR VANE CSC 12122

RADIAL DISTANCE	SETTING ANGLE	REFERENCE AIRFOIL THICKNESS	DISTANCE TO LEADING EDGE	RADII L.E.	RADII T.E.
5.5000	-21.834 -21D 50M 3S	0.0855	0.7459	0.008	0.006

LEADING EDGE AXIAL TANGENT POINT -0.4699

Q DIMENSION 0.0257 U DIMENSION 0.0230
R DIMENSION 0.0600 S DIMENSION 0.0600

STACK POINT COORDINATES 0.0 , 0.0
CENTER OF GRAVITY COORDINATES 0.3935, 0.0403
COMPRESSOR ROTATION IS COUNTER CLOCKWISE FROM THE REAR

REFERENCE COORDINATE POINTS

STATION NO.	X	Y		X	Y		X	Y
1	-0.5633*	0.1566	21	0.3647	0.0517	41	0.3792	-0.0216
2	-0.5588	0.1635	22	0.4079	0.0576	42	0.3218	-0.0319
3	-0.5139	0.1526	23	0.4509	0.0651	43	0.2752	-0.0375
4	-0.4688	0.1421	24	0.5043	0.0760	44	0.2165	-0.0413
5	-0.4127	0.1295	25	0.5466	0.0876	45	0.1692	-0.0416
6	-0.3678	0.1200	26	0.5886	0.1001	46	0.1218	-0.0395
7	-0.3229	0.1112	27	0.6404	0.1180	47	0.0634	-0.0340
8	-0.2668	0.1004	28	0.6813	0.1340	48	0.0171	-0.0282
9	-0.2220	0.0924	29	0.7317	0.1562	49	-0.0291	-0.0212
10	-0.1772	0.0849	30	0.7417	0.1613	50	-0.0866	-0.0109
11	-0.1214	0.0761	31	0.7498*	0.1558	51	-0.1324	-0.0014
12	-0.0764	0.0697	32	0.7475	0.1516	52	-0.1894	0.0121
13	-0.0204	0.0623	33	0.7387	0.1446	53	-0.2347	0.0242
14	0.0244	0.0569	34	0.6933	0.1116	54	-0.2798	0.0374
15	0.0692	0.0520	35	0.6554	0.0873	55	-0.3356	0.0554
16	0.1246	0.0463	36	0.6060	0.0595	56	-0.3799	0.0710
17	0.1634	0.0442	37	0.5650	0.0396	57	-0.4239	0.0878
18	[illegible]	0.0431	38	0.5229	0.0217	58	-0.4781	0.1102
19	0.2665	0.0440	39	0.4687	0.0024	59	-0.5210	0.1293
20	0.3104	0.0404	40	0.4244	-0.0107	60	-0.5634	0.1494

* INDICATES EXTREME POINTS

10 AUG 79 PAGE 9

FAN COMPRESSOR VANE CSC 12122

RADIAL DISTANCE	SETTING ANGLE	REFERENCE AIRFOIL THICKNESS	DISTANCE TO LEADING EDGE	RADII L.E.	RADII T.E.
6.0000	-21.296 -21D 17M 46S	0.0933	0.7450	0.008	0.006

LEADING EDGE AXIAL TANGENT POINT -0.3921

Q DIMENSION 0.0264 U DIMENSION 0.0238
R DIMENSION 0.0600 S DIMENSION 0.0600

STACK POINT COORDINATES 0.0 , 0.0
CENTER OF GRAVITY COORDINATES 0.2050, 0.0819
COMPRESSOR ROTATION IS COUNTER CLOCKWISE FROM THE REAR

REFERENCE COORDINATE POINTS

STATION NO.	X	Y		X	Y		X	Y
1	-0.4874*	0.1998	21	0.4857	0.0945	41	0.5000	0.0151
2	-0.4779	0.2070	22	0.5310	0.1002	42	0.4397	0.0047
3	-0.4309	0.1967	23	0.5761	0.1075	43	0.3908	-0.0008
4	-0.3840	0.1867	24	0.6322	0.1189	44	0.3292	-0.0042
5	-0.3254	0.1749	25	0.6768	0.1299	45	0.2797	-0.0042
6	-0.2795	0.1653	26	0.7210	0.1425	46	0.2302	-0.0016
7	-0.2317	0.1571	27	0.7758	0.1605	47	0.1693	0.0047
8	-0.1732	0.1468	28	0.8192	0.1768	48	0.1211	0.0110
9	-0.1265	0.1390	29	0.8727	0.1994	49	0.0731	0.0185
10	-0.0798	0.1316	30	0.8833	0.2043	50	0.0133	0.0293
11	-0.0214	0.1229	31	0.8917*	0.1993	51	-0.0343	0.0393
12	0.0254	0.1163	32	0.8892	0.1945	52	-0.0935	0.0532
13	0.0838	0.1086	33	0.8799	0.1872	53	-0.1406	0.0656
14	0.1305	0.1029	34	0.8318	0.1528	54	-0.1874	0.0791
15	0.1772	0.0976	35	0.7915	0.1274	55	-0.2454	0.0975
16	0.2330	0.0917	36	0.7393	0.0986	56	-0.2914	0.1134
17	0.2806	0.0886	37	0.6960	0.0779	57	-0.3371	0.1304
18	0.3262	0.0871	38	0.6515	0.0594	58	-0.3935	0.1530
19	0.3833	0.0875	39	0.5944	0.0394	59	-0.4382	0.1723
20	0.4288	0.0890	40	0.5476	0.0261	60	-0.4824	0.1927

* INDICATES EXTREME POINTS

10 AUG 79 PAGE 11

FAN COMPRESSOR VANE CSC 12122

RADIAL DISTANCE	SETTING ANGLE	REFERENCE AIRFOIL THICKNESS	DISTANCE TO LEADING EDGE	RADII L.E.	RADII T.E.
6.5000	-20.917 -20D 54M 37S	0.1012	0.7450	0.008	0.006

LEADING EDGE AXIAL TANGENT POINT -0.2396

Q DIMENSION 0.0270 U DIMENSION 0.0246
R DIMENSION 0.0600 S DIMENSION 0.0600

STACK POINT COORDINATES 0.0 , 0.0
CENTER OF GRAVITY COORDINATES 0.3180, 0.1230
COMPRESSOR ROTATION IS COUNTER CLOCKWISE FROM THE REAR

REFERENCE COORDINATE POINTS

STATION NO.	X	Y		X	Y		X	Y
1	-0.4023*	0.2436	21	0.6079	0.1372	41	0.6225	0.0516
2	-0.3932	0.2508	22	0.6551	0.1428	42	0.5595	0.0410
3	-0.3443	0.2409	23	0.7021	0.1501	43	0.5085	0.0354
4	-0.2955	0.2313	24	0.7607	0.1615	44	0.4443	0.0321
5	-0.2345	0.2198	25	0.8072	0.1726	45	0.3927	0.0324
6	-0.1858	0.2110	26	0.8535	0.1853	46	0.3412	0.0353
7	-0.1372	0.2025	27	0.9109	0.2036	47	0.2779	0.0421
8	-0.0764	0.1924	28	0.9564	0.2201	48	0.2290	0.0489
9	-0.0279	0.1847	29	1.0126	0.2431	49	0.1782	0.0568
10	0.0207	0.1773	30	1.0238	0.2491	50	0.1162	0.0682
11	0.0814	0.1685	31	1.0325*	0.2430	51	0.0669	0.0796
12	0.1299	0.1618	32	1.0298	0.2379	52	0.0055	0.0931
13	0.1908	0.1539	33	1.0201	0.2304	53	-0.0432	0.1059
14	0.2391	0.1479	34	0.9696	0.1945	54	-0.0917	0.1199
15	0.2876	0.1423	35	0.9275	0.1691	55	-0.1519	0.1388
16	0.3478	0.1359	36	0.8727	0.1391	56	-0.1996	0.1551
17	0.3944	0.1342	37	0.8274	0.1166	57	-0.2469	0.1726
18	0.4422	0.1306	38	0.7808	0.0974	58	-0.3055	0.1950
19	0.5016	0.1317	39	0.7211	0.0767	59	-0.3513	0.2156
20	0.5485	0.1326	40	0.6722	0.0629	60	-0.3977	0.2364

* INDICATES EXTREME POINTS

FAN COMPRESSOR VANE CSC 12122

RADIAL DISTANCE	SETTING ANGLE	REFERENCE AIRFOIL THICKNESS	DISTANCE TO LEADING EDGE	RADII L.E.	T.E.
7.0000	-20.611 -20D 36M 37S	0.1390	0.7450	0.008	0.006

LEADING EDGE AXIAL TANGENT POINT -0.1943

D DIMENSION 0.0276 U DIMENSION 0.0255
R DIMENSION 0.0600 S DIMENSION 0.0600

STACK POINT COORDINATES 0.0 , 0.0
CENTER OF GRAVITY COORDINATES 0.4320, 0.1637
COMPRESSOR ROTATION IS COUNTER CLOCKWISE FROM THE REAR

REFERENCE COORDINATE POINTS

STATION NO.	X	Y		X	Y		X	Y
1	-0.3160*	0.2990	21	0.7310	0.1800	41	0.7464	0.0590
2	-0.3063	0.2968	22	0.7800	0.1858	42	0.6809	0.0769
3	-0.2557	0.2807	23	0.8238	0.1932	43	0.6277	0.0710
4	-0.2090	0.2770	24	0.8896	0.2050	44	0.5609	0.0675
5	-0.1419	0.2653	25	0.9381	0.2163	45	0.5073	0.0679
6	-0.0914	0.2563	26	0.9862	0.2294	46	0.4537	0.0709
7	-0.0410	0.2476	27	1.0460	0.2482	47	0.3880	0.0781
8	0.0220	0.2373	28	1.0934	0.2652	48	0.3362	0.0852
9	0.0724	0.2244	29	1.1521	0.2890	49	0.2847	0.0935
10	0.1227	0.2218	30	1.1637	0.2941	50	0.2204	0.1055
11	0.1855	0.2127	31	1.1728*	0.2889	51	0.1693	0.1165
12	0.2358	0.2059	32	1.1700	0.2837	52	0.1058	0.1317
13	0.2936	0.1977	33	1.1599	0.2758	53	0.0553	0.1452
14	0.3469	0.1915	34	1.1075	0.2381	54	0.0051	0.1599
15	0.3992	0.1856	35	1.0637	0.2104	55	-0.0571	0.1798
16	0.4613	0.1790	36	1.0068	0.1789	56	-0.1064	0.1970
17	0.5103	0.1754	37	0.9596	0.1563	57	-0.1553	0.2153
18	0.5593	0.1734	38	0.9112	0.1361	58	-0.2158	0.2397
19	0.6206	0.1734	39	0.8490	0.1144	59	-0.2636	0.2605
20	0.6697	0.1753	40	0.7981	0.0999	60	-0.3110	0.2824

* INDICATES EXTREME POINTS

FAN COMPRESSOR VANE CSC 12122

RADIAL DISTANCE	SETTING ANGLE	REFERENCE AIRFOIL THICKNESS	DISTANCE TO LEADING EDGE	RADII L.E.	T.E.
7.5000	-20.695 -20D 41M 41S	0.1163	0.7450	0.008	0.006

LEADING EDGE AXIAL TANGENT POINT -0.0944

D DIMENSION 0.0283 U DIMENSION 0.0263
R DIMENSION 0.0600 S DIMENSION 0.0600

STACK POINT COORDINATES 0.0 , 0.0
CENTER OF GRAVITY COORDINATES 0.5461, 0.2072
COMPRESSOR ROTATION IS COUNTER CLOCKWISE FROM THE REAR

REFERENCE COORDINATE POINTS

STATION NO.	X	Y		X	Y		X	Y
1	-0.2291*	0.3408	21	0.8543	0.2251	41	0.8707	0.1265
2	-0.2193	0.3479	22	0.9050	0.2311	42	0.8025	0.1147
3	-0.1668	0.3375	23	0.9556	0.2389	43	0.7472	0.1085
4	-0.1144	0.3273	24	1.0187	0.2512	44	0.6777	0.1049
5	-0.0490	0.3152	25	1.0689	0.2632	45	0.6220	0.1053
6	0.0033	0.3058	26	1.1188	0.2769	46	0.5662	0.1087
7	0.0555	0.2968	27	1.1508	0.2968	47	0.4981	0.1164
8	0.1207	0.2860	28	1.2300	0.3148	48	0.4445	0.1240
9	0.1729	0.2777	29	1.2909	0.3399	49	0.3910	0.1329
10	0.2248	0.2695	30	1.3030	0.3453	50	0.3245	0.1458
11	0.2899	0.2603	31	1.3124*	0.3396	51	0.2716	0.1574
12	0.3420	0.2530	32	1.3096	0.3346	52	0.2059	0.1736
13	0.4070	0.2444	33	1.2992	0.3262	53	0.1537	0.1880
14	0.4591	0.2378	34	1.2453	0.2862	54	0.1019	0.2036
15	0.5111	0.2315	35	1.2000	0.2567	55	0.0376	0.2247
16	0.5754	0.2244	36	1.1411	0.2232	56	-0.0133	0.2430
17	0.6259	0.2205	37	1.0923	0.1991	57	-0.0637	0.2624
18	0.6766	0.2184	38	1.0420	0.1777	58	-0.1261	0.2883
19	0.7401	0.2183	39	0.9774	0.1546	59	-0.1754	0.3104
20	0.7909	0.2202	40	0.9245	0.1391	60	-0.2241	0.3336

* INDICATES EXTREME POINTS

FAN COMPRESSOR VANE CSC 12122

RADIAL DISTANCE	SETTING ANGLE	REFERENCE AIRFOIL THICKNESS	DISTANCE TO LEADING EDGE	RADII L.E.	RADII T.E.
3.0000	-21.285 -21D 17M 6S	0.1248	0.7450	0.008	0.006

LEADING EDGE AXIAL TANGENT POINT 0.0118

Q DIMENSION 0.0289 U DIMENSION 0.0271
R DIMENSION 0.0600 S DIMENSION 0.0600

STACK POINT COORDINATES 0.0 , 0.0
CENTER OF GRAVITY COORDINATES 0.6594, 0.2576
COMPRESSOR ROTATION IS COUNTER CLOCKWISE FROM THE REAR

REFERENCE COORDINATE POINTS

STATION NO.	X	Y		X	Y		X	Y
1	-0.1436*	0.4029	21	0.9772	0.2762	41	0.9951	0.1708
2	-0.1337	0.4098	22	1.0296	0.2827	42	0.9240	0.1580
3	-0.0794	0.3984	23	1.0620	0.2912	43	0.8664	0.1514
4	-0.0252	0.3874	24	1.1473	0.3046	44	0.7939	0.1475
5	0.0425	0.3742	25	1.1992	0.3176	45	0.7357	0.1480
6	0.0966	0.3641	26	1.2509	0.3326	46	0.6777	0.1518
7	0.1506	0.3543	27	1.3150	0.3542	47	0.6069	0.1603
8	0.2181	0.3426	28	1.3658	0.3738	48	0.5513	0.1687
9	0.2720	0.3336	29	1.4287	0.4012	49	0.4959	0.1784
10	0.3259	0.3247	30	1.4412	0.4071	50	0.4270	0.1924
11	0.3932	0.3146	31	1.4511*	0.4015	51	0.3723	0.2051
12	0.4471	0.3067	32	1.4483	0.3963	52	0.3043	0.2227
13	0.5145	0.2973	33	1.4377	0.3872	53	0.2503	0.2382
14	0.5684	0.2901	34	1.3827	0.3440	54	0.1968	0.2551
15	0.6223	0.2833	35	1.3363	0.3121	55	0.1305	0.2779
16	0.6833	0.2755	36	1.2757	0.2758	56	0.0780	0.2977
17	0.7410	0.2712	37	1.2252	0.2497	57	0.0261	0.3186
18	0.7933	0.2639	38	1.1731	0.2264	58	-0.0381	0.3466
19	0.8539	0.2637	39	1.1061	0.2013	59	-0.0887	0.3704
20	0.9115	0.2708	40	1.0511	0.1845	60	-0.1387	0.3955

* INDICATES EXTREME POINTS

FAN COMPRESSOR VANE CSC 12122

RADIAL DISTANCE	SETTING ANGLE	REFERENCE AIRFOIL THICKNESS	DISTANCE TO LEADING EDGE	RADII L.E.	RADII T.E.
3.5000	-22.794 -22D 47M 37S	0.1329	0.7450	0.008	0.007

LEADING EDGE AXIAL TANGENT POINT 0.1274

Q DIMENSION 0.0294 U DIMENSION 0.0279
R DIMENSION 0.0600 S DIMENSION 0.0600

STACK POINT COORDINATES 0.0 , 0.0
CENTER OF GRAVITY COORDINATES 0.7694, 0.3233
COMPRESSOR ROTATION IS COUNTER CLOCKWISE FROM THE REAR

REFERENCE COORDINATE POINTS

STATION NO.	X	Y		X	Y		X	Y
1	-0.0640*	0.4823	21	1.0981	0.3393	41	1.1170	0.2269
2	-0.0538	0.4897	22	1.1524	0.3462	42	1.0423	0.2136
3	0.0024	0.4774	23	1.2067	0.3554	43	0.9818	0.2070
4	0.0588	0.4655	24	1.2742	0.3702	44	0.9057	0.2040
5	0.1288	0.4513	25	1.3279	0.3847	45	0.8447	0.2058
6	0.1848	0.4403	26	1.3813	0.4017	46	0.7840	0.2112
7	0.2408	0.4296	27	1.4473	0.4262	47	0.7115	0.2209
8	0.3107	0.4169	28	1.4995	0.4486	48	0.6537	0.2302
9	0.3666	0.4071	29	1.5639	0.4799	49	0.5962	0.2408
10	0.4225	0.3977	30	1.5767	0.4867	50	0.5248	0.2561
11	0.4923	0.3864	31	1.5873*	0.4811	51	0.4680	0.2699
12	0.5482	0.3777	32	1.5846	0.4759	52	0.3978	0.2891
13	0.6180	0.3673	33	1.5741	0.4658	53	0.3418	0.3060
14	0.6740	0.3594	34	1.5188	0.4178	54	0.2864	0.3242
15	0.7299	0.3518	35	1.4717	0.3823	55	0.2180	0.3489
16	0.8001	0.3429	36	1.4095	0.3420	56	0.1638	0.3702
17	0.8539	0.3370	37	1.3574	0.3131	57	0.1103	0.3928
18	0.9079	0.3335	38	1.3033	0.2874	58	0.0443	0.4229
19	0.9757	0.3344	39	1.2334	0.2598	59	-0.0078	0.4485
20	1.0301	0.3340	40	1.1758	0.2416	60	-0.0591	0.4754

* INDICATES EXTREME POINTS